

Response to Anonymous Referee #1

General comments

Author Response: We appreciate the careful review and constructive suggestions. Our point-by-point responses to the reviewer's general and specific comments are presented below. The changes to the initial manuscript text and supplement illustrations are marked in red.

This paper uses fast roadside measurements of a range of gaseous and particulate emissions for heavy-duty vehicles in Sweden. A relatively large sample size of measurements is used to infer the emission characteristics of different vehicle types-mostly by Euro status. The paper provides an up to date understanding of the evolution of emissions of important species that include non-regulatory species. The paper is generally well-written but perhaps lacks a clear explanation of what the new findings are

and how they differ from previous work. Indeed, the size of Table 1 and 2 indicate that a considerable amount of work has been carried out before in this area. Nevertheless, emissions from road vehicles continually evolve and on balance I think this study does contribute some useful, up to date emissions from an important class of vehicles.

1. Line 254 where it is stated non-Swedish trucks tend to have higher emissions. I think this statement needs to be more robust. As the authors point out, there is no Euro class information for non-Swedish trucks (and therefore no knowledge of the numbers in each Euro class). Given the large range of emissions by Euro status, I don't think this statement is particularly defensible. Furthermore, all the data shown in Table 1/2 I think have overlapping 95% CI when making this comparison. Also, the statement "which may be attributed to the more stringent domestic goals regarding pollution, clean air, greenhouse gas emissions, energy efficiency, and innovative sustainable solutions..." is vague. Is it the case that Swedish annual technical inspections are more stringent than other countries? I doubt there is evidence for that.

Author Response: We agree that the lack of Euro type information of non-Swedish HDTs indeed makes the direct comparison between the emission factors of Swedish HDTs and non-Swedish HDTs of different Euro types difficult. Based on the reviewer's comments, we considered the Swedish and non-Swedish HDTs as two major categories to compare if there are significant differences between their emission factors. We believe such comparison is useful for readers given that the non-Swedish HDTs contribute to 32% of the vehicles we studied. Since the emission data are not normally distributed, statistical significance between EF distribution of total Swedish and non-Swedish HDTs is assessed with the Kolmogorov-Smirnov test. Table R1 compares the average and median emission data and lists the p-values from the Kolmogorov-Smirnov test. The p-values are calculated at the statistical 95% confidence level. Overall, compared with non-Swedish HDTs, Swedish HDTs generally have a lower median and average EF_{NOx} but there are no significant differences in the EF of other pollutants.

Author action: Accordingly, we revised line 328 to 332 in the revised manuscript (332 to 335 in the marked-up manuscript) from "Compared with non-Swedish HDTs, Swedish HDTs generally have lower EFs in terms of all the pollutants (Fig. 2 and Tables 1 and 2), which may be attributed to the more stringent domestic goals regarding pollution, clean air, greenhouse gas emissions, energy efficiency, and innovative sustainable solutions (Government Offices of Sweden, 2017). One may note that the non-Swedish HDTs was not identified according to Euro class and could contain a larger share of non-Euro VI trucks." to:

“Compared with the fleet of non-Swedish HDTs, the Swedish HDT fleet generally have a lower median and average EF_{NO_x} but there are no significant differences in the EF of other pollutants (Fig. 2 and Tables 1 and 2). The differences in EF_{NO_x} are significant at the statistical 95% CI using the Kolmogorov-Smirnov test, used in favour to typical student t-test to account for non-normality of the EF distributions. As information of Euro class, engine types and treatment technologies of non-Swedish HDTs is not available, we cannot further explore why there is a difference between the two fleets.”

Table R1. Comparison of the average and median emission data for PM, PN, BC, NO_x , CO and HC from the Swedish and non-Swedish HDTs and p-values from Kolmogorov-Smirnov test.

Pollutant	Average EF		Median EF		<i>p</i>
	Swedish	Non-Swedish	Swedish	Non-Swedish	
PM	95.9 mg (kg fuel) ⁻¹	117.3 mg (kg fuel) ⁻¹	8.1 mg (kg fuel) ⁻¹	16.4 mg (kg fuel) ⁻¹	0.17
PN	9.6×10 ¹⁴ # (kg fuel) ⁻¹	11.1×10 ¹⁴ # (kg fuel) ⁻¹	1.7×10 ¹⁴ # (kg fuel) ⁻¹	1.7×10 ¹⁴ # (kg fuel) ⁻¹	0.95
BC	110.9 mg (kg fuel) ⁻¹	150.0 mg (kg fuel) ⁻¹	2.4 mg (kg fuel) ⁻¹	3.2 mg (kg fuel) ⁻¹	0.25
NO_x	10.7 g (kg fuel) ⁻¹	13.0 g (kg fuel) ⁻¹	2.7 g (kg fuel) ⁻¹	6.3 g g (kg fuel) ⁻¹	0.01
CO	18.6 g (kg fuel) ⁻¹	19.1 g (kg fuel) ⁻¹	14.5 g (kg fuel) ⁻¹	13.4 g (kg fuel) ⁻¹	0.98
HC	0.9 g (kg fuel) ⁻¹	0.9 g (kg fuel) ⁻¹	0 g (kg fuel) ⁻¹	0 g (kg fuel) ⁻¹	0.57

2. How sure can the authors be that certain Euro classes of vehicles have certain technologies fitted? For example, is it known that any of the tested vehicles were retrofitted in some way?

Author Response: We do not have specific information on after-treatment systems for each HDT in this study. We referred to the International Council for Clean Transportation (ICCT) which reported that Particulate Filters (DPFs) are required to comply with PM and PN for Euro VI HDTs (Williams and Minjares, 2016). No information about potential retrofits of tested HDTs was available for the vehicles measured in this study.

3. Where comments are made about decreases (or changes in general) I think it is important to provide the corresponding uncertainty. It seems that in many cases that there will be overlapping confidence intervals and therefore important to convey where differences are statistically clear or not.

Author Response: Thanks for your suggestions. We have conducted the Jonckheere-Terpstra test to determine if there is a statistically significant trend of pollutant emission factors based on the different Euro classes.

The null hypothesis for the Jonckheere-Terpstra test is that the distribution of pollutant emission factors is the same across the categories of Euro classes and the alternative hypothesis is that pollutant median EF decreases with more stringent Euro standards. The p-values were calculated at the statistical 95% confidence interval. The Jonckheere-Terpstra test for ordered alternatives shows that there were statistically significant trends of lower median EF_{PM} , EF_{PN} , EF_{BC} , EF_{NO_x} , and EF_{CO} with more stringent Euro standards from Euro III to Euro VI HDTs. However, no significant decreasing trend was evident for EF_{HC} from Euro III to Euro VI HDTs. These test results are consistent with the statements we made in the main text.

Author action: We have added the following additions to the previous sentences.

Line 195-197 in the revised manuscript (198-200 in the marked-up manuscript): Added two sentences, this section now reads “Generally, both PM and PN emissions decreased with more stringent Euro emission standards, and especially for Euro VI where larger changes in emission characteristics were evident. These decreasing trends are statistically significant at the 95% CI using the Jonckheere-Terpstra test, a nonparametric test for trends in ordered groups. In addition to PM and PN, the emission trends of BC, NO_x, CO and HC with respect to the level of stringency of Euro standards were statistically examined.”

Line 247-249 in the revised manuscript (248-250 in the marked-up manuscript). The sentence has been revised from “The BC emissions generally showed an overall decrease when moving towards newer Euro classes, which is similar to the EF_{PM} trend with the exception of Euro IV HDTs.” to “The BC emissions generally showed a decrease from Euro III to Euro VI HDTs (Jonckheere-Terpstra test, $p<0.01$), which is similar to the EF_{PM} trend with the exception of Euro IV HDTs.”

Line 287-288 in the revised manuscript (289-290 in the marked-up manuscript): The sentence has been revised from “Generally, both EF_{PM} and EF_{PN} exhibited a decreasing trend from Euro III to Euro IV and from Euro V to EEV HDTs.” to “Generally, both EF_{PM} and EF_{PN} exhibited a decreasing trend from Euro III to Euro IV and from Euro V to EEV HDTs (Jonckheere-Terpstra test, $p<0.01$).”

Line 322-324 in the revised manuscript (325-326 in the marked-up manuscript): The sentence has been revised from “HC emission was relatively low for all HDT types, but no obvious decreasing trend was evident for EF_{HC} from Euro III to Euro VI HDTs (Fig. S8d and Table 2).” to “HC emission was relatively low for all HDT types, and no obvious decreasing trend was evident for EF_{HC} from Euro III to Euro VI HDTs (Jonckheere-Terpstra test, $p=0.895$) (Fig. S8d and Table 2).”

Line 427-430 in the revised manuscript (435-437 in the marked-up manuscript): The sentences have been revised from “Particle emissions of PM, BC and to a lesser extent PN exhibited substantial reductions from Euro III to Euro VI HDTs. The gaseous emissions of NO_x and CO also showed significant decrease with respect to Euro class, while the HC emission was relatively low for all the HDT Euro class types.” to “Particle emissions of PM, BC and to a lesser extent PN exhibited substantial reductions from Euro III to Euro VI HDTs (Jonckheere-Terpstra test, $p<0.01$). The gaseous emissions of NO_x and CO also showed a significant decrease with respect to Euro class (Jonckheere-Terpstra test, $p<0.01$), while the HC emission was relatively low for all the HDT Euro class types.”

4. How was the sigma of the background component of CO₂ calculated? This was not based on upwind measurements, right? Presumably the variation in background cannot be represented by a single value and it varies also. Some more details are needed. It would be helpful to have a Figure that shows a 'typical' peak being analysed showing the concentration of CO₂ and all other species. This would also help demonstrate that a measurement frequency of ~1 Hz is sufficient to capture an individual vehicle plume. Moreover, a discussion on the effect of sampling rate (and potentially different sampling rates) on the extracted plume characteristics / metrics would be beneficial.

Author Response and action: Please see Fig.1 in the main text where some examples of typical temporal profiles of CO₂ and pollutant concentrations in the plumes are given. The CO₂ concentration was measured by a non-dispersive infrared gas

analyser operated at 1Hz. CO₂ concentration for each plume was integrated and subtracted by the background CO₂ concentration to obtain the peak areas of CO₂, which were used to represent different degrees of dilution during sampling. The background CO₂ concentration $[CO_2]_{t_1}$ of each individual CO₂ peak was calculated by averaging five concentration data points just before the peak start point t_1 . Plume pollutant concentrations were integrated and normalized by the peak area of CO₂ concentration to calculate corresponding pollutant emission factors of individual HDTs to compensate for different dilution levels, as expressed in Eq. (1):

$$EF_{pollutant} = \frac{\int_{t_1}^{t_2} ([pollutant]_t - [pollutant]_{t_1}) dt}{\int_{t_1}^{t_2} ([CO_2]_t - [CO_2]_{t_1}) dt} \times EF_{CO_2} . \quad (1)$$

In this study, all instruments operated at a time resolution of 1s (1Hz) or faster, which is sufficiently fast to measure pollutant concentration peaks (typically 5 to 20 s in duration) as shown in Fig. 1c-e. Thus, we do not think it would be needed to discuss this further. However, we added this statement to line 148-150 in the revised manuscript and the marked-up manuscript, from “All the instruments were operated at least at 1Hz of sampling frequency to capture rapidly changing concentrations during the passage of a HDT.” to “All the instruments were at least operated at 1Hz of sampling frequency to capture rapidly changing concentrations during the passage of a HDT, which is sufficiently fast to measure pollutant concentration peaks (typically 5 to 20 s in duration) as shown in Fig. 1c-e.”

We have compared the peak shapes under the different sampling frequency conditions by averaging 1Hz data to 2s, 3s, 4s, 5s intervals respectively. Low sampling frequencies may produce distortions to the concentration peaks (Fig. R1). For a narrow peak such as CO₂, lower sampling frequencies can cause difficulties in identifying the peak position and shape. These may result in calculation errors in integrated peak areas.

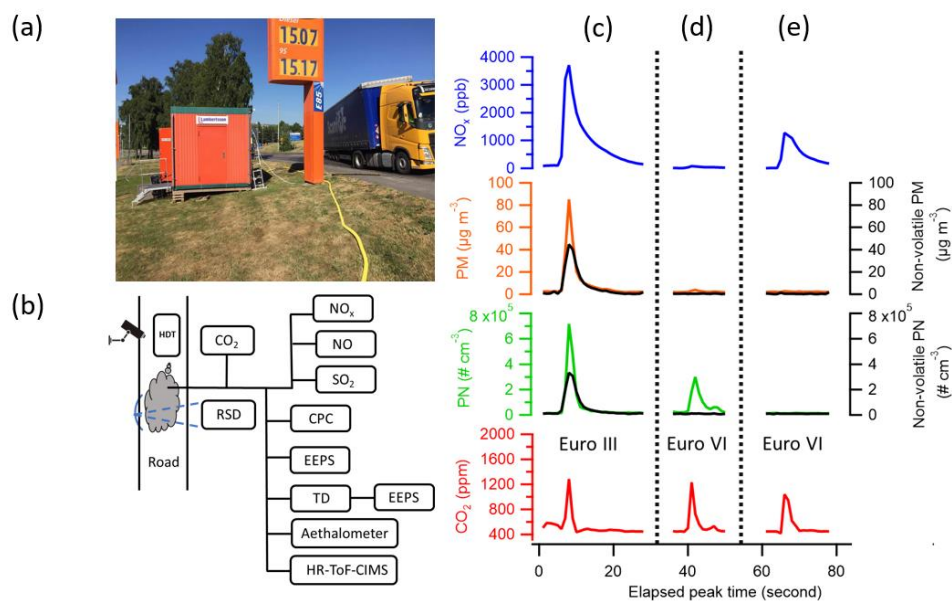


Figure 1. (a) Sampling site at the roadside in Gothenburg, Sweden, (b) schematic of the experimental set-up. HDT (Heavy-duty truck), RSD (Remote Sensing Device), CPC (Condensation Particle Counter), EEPS (Engine Exhaust Particle Sizer Spectrometer), TD (Thermodenuder) and HR-ToF-CIMS* (High-Resolution Time-of-Flight Chemical Ionization Mass Spectrometer) and examples of signals from three passing HDTs. Concentrations of CO₂, PN, non-volatile PN, PM, non-volatile PM, and NO_x from (c) a typical Euro III HDTs and (d) a typical Euro VI HDTs and (e) a Euro VI HDTs with low PN emission. *The data from the HR-ToF-CIMS will be presented elsewhere.

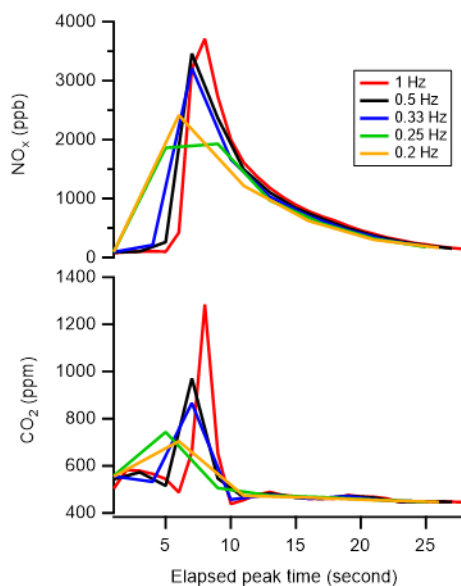


Figure R1. Concentrations of CO₂ and NO_x from a HDT measured under different sampling frequencies

5. Do the authors have any information about the engine type or manufacturer to understand whether that is an important factor that could explain some of the differences observed? Earlier on in the text it is stated that these types of factor can be important in determining emissions, so it would be useful to explain this. Similarly, is there any difference in the size of vehicle sampled (e.g. by engine size or kerb weight)?

Author Response: We have also investigated pollutant emission trends with respect to different manufacturers. Pollutant emission factors of HDTs under the same Euro class but from different manufacturers are compared in Fig. S9. The red solid lines in Fig. S9 represent the median EFs for the different engine manufacturers.

Author action: A discussion section on the influence of individual vehicle manufacturers has been added to Sect. 3.3 in the main text and Fig. S9 has been added to the supplemental materials. The following has been added, starting on line 333 in the revised manuscript (line 341 in the marked-up manuscript):

“In addition to engine Euro type, pollutant emission trends were also investigated with respect to five different vehicle manufacturers (M1, M2, M3, M4, and M5). EF_{PM} , EF_{PN} , EF_{BC} and EF_{NOx} of HDTs under the same Euro class but from different manufacturers are compared in Fig. S9. Since EF data was not normally distributed, statistical significance is assessed with a Kruskal–Wallis test. It is a non-parametric analogue of the one-way ANOVA test. The p-values are calculated at the statistical 95% confidence level. No significant group difference ($p>0.05$) was observed in EF_{PM} , EF_{PN} , EF_{BC} , and EF_{NOx} for Euro V HDTs, i.e., HDTs from five different manufacturers show comparable emission characteristics. EF_{PM} , EF_{PN} , and EF_{NOx} of Euro VI HDTs show no dependency on manufacturers, but a significant difference was observed between M2 and M5 in EF_{BC} of Euro VI HDTs ($p=0.016$). (No analysis on Euro III, Euro IV, and EEV HDTs was conducted due to the limited vehicle number from each manufacturer).”

In this study, engine size and kerb weight information were not available. However, the related information that whether the HDT is equipped with a container or not can be accessed by the captured photo, but the loading information of the container (full or empty) is not known. We conducted a Kolmogorov-Smirnov (at 0.05 significance level) test to compare the cumulative distribution of the pollutant emission factors of HDTs with and without containers. No significant difference between EF_{PM} , EF_{PN} , EF_{BC} and EF_{NOx} of HDTs with and without a container ($p>0.05$) was observed.

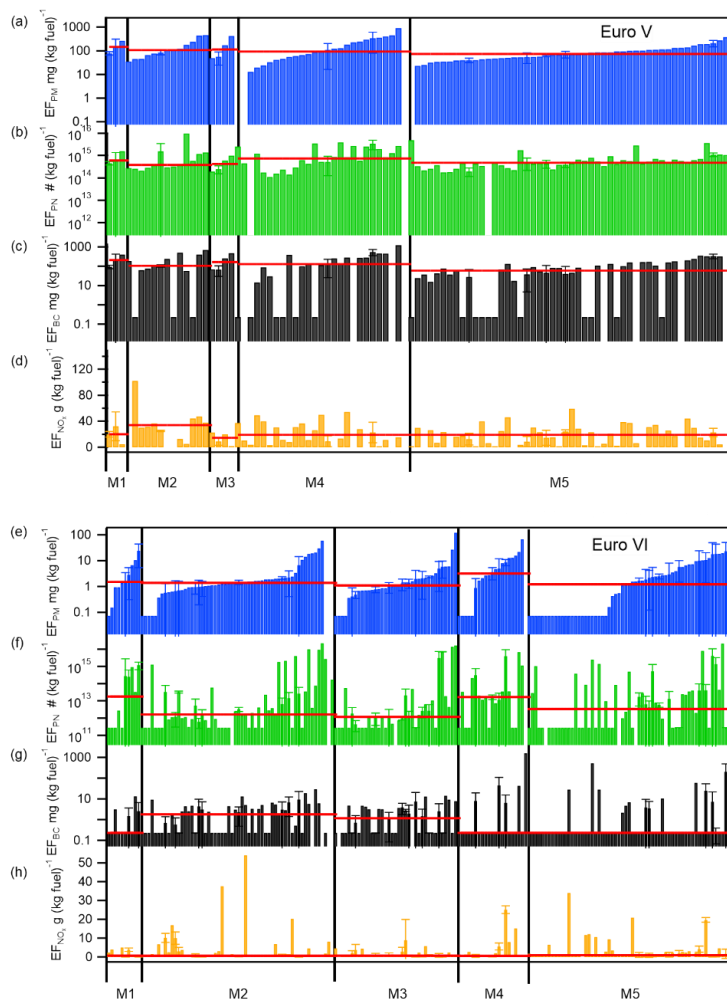


Fig. S9. (a) EF_{PM} , (b) EF_{PN} , (c) EF_{BC} and (d) EF_{NOx} for Euro V HDTs and (e) EF_{PM} , (f) EF_{PN} , (g) EF_{BC} and (h) EF_{NOx} for Euro VI HDTs with respect to manufacturers: M1, M2, M3, M4 and M5. For an individual HDT with multiple passages, an average has been calculated and the error given is the standard deviation (1σ). The red solid lines represent the median EFs for the different engine manufacturers. Kruskal–Wallis test shows no significant manufacturer difference in EF_{PM} , EF_{PN} , EF_{BC} and EF_{NOx} for Euro V HDTs, whereas a significant difference was observed between M2 and M5 in EF_{BC} of Euro VI HDTs ($p=0.016$).

6. Section 4 (Atmospheric implications and conclusions) does not actually consider the atmospheric implications. I think it should – and if it did – it would strengthen the paper. For example, it would be useful to consider the implications for near-road exposures and consider how UFP could evolve through coagulation etc. as plumes disperse away from roads. Reducing PM mass is clearly important but if the consequence in doing so increase PN, then that could be important.

Author response and action: Thanks for the review's constructive suggestion, which can help us improve the value of our study. We have added the related discussions about implications in Sect.4.

“Reducing particle mass by DPF is clearly important but the consequence in doing so removes particle surface area available for condensation and may therefore favour nucleation mode particle formation if not the precursors of these are also reduced. Furthermore, due to the absence of larger particles, the coagulation rate is decreased and produced nucleation mode particle can retain for a longer time in the atmosphere, which has a direct influence on the evaluation of near-road human exposure.”

References

Williams, M., and Minjares, R.: A technical summary of Euro 6/VI vehicle emission standards, International Council for Clean Transportation (ICCT), Washington, DC, accessed July, 10, 2017, 2016

Response to Anonymous Referee #2

General comments

Author Response: We thank the referee for the positive and insightful comments. Our point-by-point responses to the reviewer's general and specific comments are presented below. The changes to the initial manuscript text and supplement illustrations are marked in red. Any page or paragraph reference is to the original manuscript and the reviewers' original comments are in *italic*. The manuscript has been updated accordingly.

This study reports roadside measurements of 556 heavy-duty trucks in Sweden. The paper uses these measurements to investigate how several pollutants of interest vary by each truck's Euro pollutant emissions standard and carries out several additional analyses including the skewness of the distribution of emitters. In addition, the study does a very extensive comparison to past relevant literature. I think the paper is a valuable contribution to the literature and should be published after considering the comments below. The comments below that I think require the most attention have to do with adding additional analysis or at least discussion on how various amounts of exhaust dilution paper impact your particle number emission factors. This includes both variability in dilution among different trucks in your measurements, and especially differences between your study and the past work used for comparison.

1. Line 104: Please consider adding a short statement here related to how the uphill conditions could impact results. You discuss this later in the paper, but you might want to alert the reader to this, and point to where you discuss it.

Author Response and action: Thanks for your suggestion, we have added a statement at the suggested position in the text (line 104 in the revised manuscript and the marked-up manuscript):

“Pollutant emissions from HDTs were measured at a roadside location in Gothenburg, Sweden (Fig. 1). The HDTs passed the sampling location with an average speed of 27 km h⁻¹ and acceleration of 0.7 km h⁻¹ s⁻¹ on a slight uphill slope (~2°). **Under such uphill driving conditions, vehicles are expected to emit higher levels of pollutants than during downhill and cruise driving. This will be further examined in Sect. 3.3.**”

2. Line 163: Please discuss how you chose t1 and t2 for the integration. And more importantly, how did you deal with the different plume widths for NOx versus other pollutants? How sensitive are results to chosen t1 and t2?

Author Response: In previous applications of this peak integration method to characterize particle and gaseous pollutant emission factors for heavy-duty diesel trucks, t₁ and t₂ were determined by identifying inflection points to the left and right of the individual pollutant peaks (Dallmann et al., 2011; Preble et al., 2015). A similar method was used here, examples of chosen t₁ and t₂ are given in Fig. R1.

Author action: We have added a statement after line 166 in the revised manuscript (line 168 in the marked-up manuscript) “The time interval of t₁ to t₂ represents the period when the instruments measured the concentration of an entire pollutant peak from an individual HDT (see Fig. 1c-e). Dallmann et al. (2011) and Preble et al. (2015) used the concepts of inflection points to identify t₁ and t₂. In our study, t₁ and t₂ were determined similarly: t₁ is the point before the pollutant concentration intensity increases abruptly and t₂ is when the intensity becomes relatively flat and undistinguishable compared to background levels.

It is noted that the integrated peak intensity is insensitive to the exact location of t_2 since the added integrated signals at or beyond this point are fluctuating around zero. t_1 and t_2 were determined independently of each pollutant peak to account for differences in the time response of individual instruments to the exhaust plume.”

If we use the same t_1 and t_2 for different pollutants, the integrated peak area would be biased, so the choices of t_1 and t_2 are sensitive to the peak width, or more specifically pollutant type.

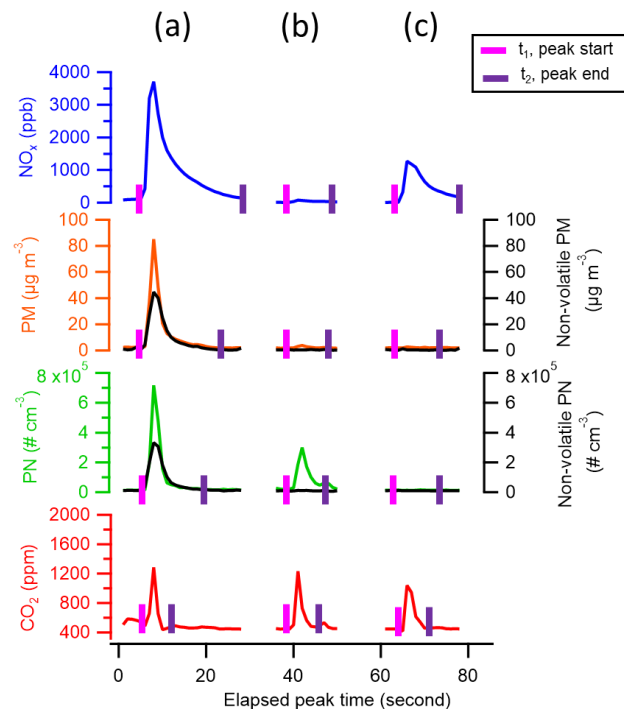


Figure R1. Concentrations of CO₂, PN, non-volatile PN (black line), PM, non-volatile PM (black line), and NO_x from (a) a typical Euro III HDT and (b) a typical Euro VI HDT and (c) a Euro VI HDT with low PN emission.

3. Line 188-200: See major comments above. PN measurements would be highly dependent on the amount of dilution the plume has undergone between the engine and the measurement. I would imagine this would contribute to differences between your measured emission factors and emission standards. What are the dilution requirements when certifying for Euro standards?

Line 200-202: Could variability in dilution contribute to the scatter too? Please think this through for all sections that discuss PN emissions results.

Author Response: To compensate for different dilution levels, particle emissions from individual HDTs were normalized by the CO₂ concentration as illustrated in Eq. (1).

$$EF_{\text{pollutant}} = \frac{\int_{t_1}^{t_2} ([\text{pollutant}]_t - [\text{pollutant}]_{t_1}) dt}{\int_{t_1}^{t_2} ([\text{CO}_2]_t - [\text{CO}_2]_{t_1}) dt} \times EF_{\text{CO}_2} . \quad (1)$$

In principle, EFs calculated by Eq. (1) would not be dependent on the amount of dilution the plume has undergone between the engine and the measurement if there is no transformation of the pollutants. Nowadays, the legislation in Europe prescribes the Constant Volume Sampling (CVS) as the reference sampling for particle emission certification, in which the sample mixed gas of exhaust and diluent gas is controlled to have a constant flow rate. The dilution ratio has been left out of direct regulation and is only implicitly controlled by the need to achieve sufficient exhaust cooling before particle sampling (Ntziachristos et al., 2004). The regulations regarding PN is following the PMP protocol, where only the solid particle fraction $> 23 \text{ nm}$ is accounted for, hence a fraction that is less sensitive to the dilution.

However, the effective emission of all nucleation mode particles is depending on nucleation, coagulation, and evaporation that could be happening on the time scale of the dilution and cooling of the exhaust gases. The relationship between the number emission factor of nucleation mode particles and CO_2 peak areas are shown in Fig. R2. Higher CO_2 concentrations indicated a lower dilution level. Since EF data was not normally distributed, the strength and direction of the association between nucleation mode particle number emission factors and CO_2 peak areas were assessed with the Kendall's tau-b correlation. It is a nonparametric alternative to the Pearson's correlation. The p-values are calculated at the 95% confidence level. Intuitively, one would expect that lowering dilution, i.e., increased observed CO_2 concentrations, might result in a higher EF_{PN} in nucleation mode. However, as shown in Fig R2, no significant enhancement of the formation of nucleation mode particles was evident under lower dilution levels and the nucleation mode particle number emission factors remained practically constant for all Euro III-V HDTs ($p > 0.05$) while Euro VI HDTs showed a weak negative correlation (correlation coefficient of -0.3 , $p < 0.01$), i.e. opposite to what could be expected from coagulation/evaporation. This demonstrates that any potential dilution effect on the variability of the measurements was limited and well represents typical dilution one observes at kerb-sites.

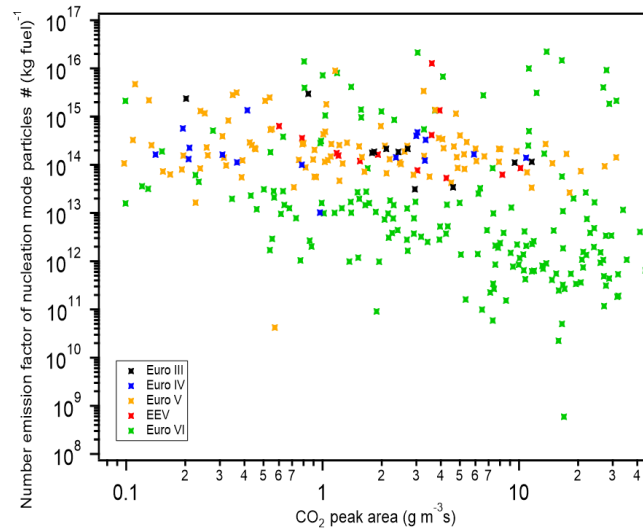


Figure R2. The relationship between number emission factor of nucleation mode particles and CO_2 peak areas

4. Line 240-241: Please make sure to include text in figure captions when you are not including data from all trucks. Are you sure that leaving these data out doesn't lead to a problem with biasing the results? I would imagine that if you are not including results for trucks that have measured concentrations below measurement detection limits, you'd be leaving out the cleanest trucks (though could also be due to the plume missing the sample line). Please think this through for all sections that report results that remove trucks with measurements below detection limits.

Author Response: Thanks for the suggestion. We have added the description of the excluded data in the figure captions. We apologize for the confusion caused; we indeed included the emission data lower than the set detection limit (four times the standard deviation of the pollutant background signal) into the analysis throughout the whole manuscript. As we mentioned in Sect. 2.3, emission factors for plumes with pollutant concentrations lower than our set detection limit were replaced by the minimum value among all recorded emission factors (EF_{min}) rather than being omitted to avoid inflating emissions from low-emitting HDTs. The concentration data below the detection limits were removed from the figure only for the purpose of a clearer figure presentation.

Author action: We have added the following statement after line 253-254 in the revised manuscript (255-256 in the marked-up manuscript):

“HDTs with either EF_{NO_2} or EF_{NO_x} lower than the detection limits of the instruments were removed in Fig. 2d for illustration purposes, while all the presented statistical analyse include all the data as outlined above.”

5. Table 1: I don't understand how you've categorized this table. For example, I see studies in this table that are not performed in Europe but are under the Euro VI category. Also, I noticed papers that you are citing in the study and that have emission factor results, but are not in this table. Please ensure you have considered all relevant studies.

Author Response action: Thanks for review's suggestions. We have rearranged some rows in Table 1 and Table 2 and separated the studies of non-European HDV emissions with Euro VI HDV emissions in each Table. Additionally, more emission factor results have been added to the tables.

Table 1. Comparison of the average emission data^a for PM and PN from the present study with literature data.

PM/PN						
Vehicle type	Speed km h ⁻¹	Dp range nm	Method	Instrument	EF_{PM} mg (kg fuel) ⁻¹	EF_{PN} # (kg fuel) ⁻¹ 10 ¹⁴
Euro III HDT in this study	26±6 ^b	5.6-560	roadside	EEPS	684±365	20.3±11.7
Euro III bus (Hallquist et al., 2013)	acceleration	5.6-560	roadside	EEPS	6.7-2074	0.11-45
	constant speed	5.6-560	roadside	EEPS	151-273	0.12-4.2
Euro III bus with DPF (Hallquist et al., 2013)	acceleration	5.6-560	roadside	EEPS	62-2465	1.9-23
	constant speed	5.6-560	roadside	EEPS	41-142	1.1-9.7
Euro III bus	≤25	PM ₁	plume chasing	ELPI ^c	1240±220 ^b	

(Pirjola et al., 2016)	(bus depot)	$D_p \geq 2.5$		CPC		20.6 ± 3.2^b
	≤ 45	PM_1	plume chasing	ELPI ^c	500	
	(bus line)	$D_p \geq 2.5$		CPC		17.7
Euro III bus with DPF+SCR (Watne et al., 2018)	acceleration	5.6-560	roadside	EEPS	8.9 ± 0.2	0.12 ± 0.12
Euro III bus with DPF+SCR (Liu et al., 2019)	stop and go (bus stop)	5.6-560	roadside	EEPS	30 ± 26^b	14.0 ± 3.0^b
Euro III diesel bus and truck (Zavala et al., 2017)	driving cycle	35-1000	plume chasing & roadside	SP-AMS ^f	4300	-
Euro IV HDT in this study	23 ± 8^b	5.6-560	roadside	EEPS	172 ± 68	8.7 ± 3.0
Euro IV bus with EGR (Hallquist et al., 2013)	acceleration	5.6-560	roadside	EEPS	562-3089	13-44
	constant speed	5.6-560	roadside	EEPS	91-489	5.8-47
Euro IV bus with EGR+DPF (Hallquist et al., 2013)	acceleration	5.6-560	roadside	EEPS	177-650	5.1-13
	constant speed	5.6-560	roadside	EEPS	58-61	2.6-3.1
Euro IV bus with EGR+DPF (Pirjola et al., 2016)	≤ 25	PM_1	plume chasing	ELPI ^c	1190 ± 520^b	
	(bus depot)	$D_p \geq 2.5$		CPC		8.9 ± 1.6^b
Euro IV bus with SCR (Watne et al., 2018)	acceleration	5.6-560	roadside	EEPS	145-560	3-13
Euro IV diesel bus and truck (Zavala et al., 2017)	driving cycle	35-1000	plume chasing and roadside	SP-AMS ^f	1800	-
Euro V HDT in this study	27 ± 7^b	5.6-560	roadside	EEPS	146 ± 49	9.7 ± 2.7
Euro V bus+SCR (Hallquist et al., 2013)	acceleration	5.6-560	roadside	EEPS	125-766	4.4-92
	constant speed	5.6-560	roadside	EEPS	41-509	2.7-33
Euro V bus (Watne et al., 2018)	acceleration	5.6-560	roadside	EEPS	145 ± 70	3.0 ± 1.7
Euro V HDV with SCR (Rymaniak et al., 2017)	average at 45	PM_1 / 5.6-560	PEMS	MSS ^e	1840^d	
				EEPS		0.09^d
Euro V bus with SCR (Liu et al., 2019)	stop and go (bus stop)	5.6-560	roadside	EEPS	180 ± 15^b	6.5 ± 2.9^b
Euro V diesel bus and truck (Zavala et al., 2017)	driving cycle	35-1000	plume chasing and roadside	SP-AMS ^f	720	-
EEV HDT in this study	25 ± 8^b	5.6-560	roadside	EEPS	78 ± 35	16.5 ± 23.6
EEV bus with EGR +DPF (Pirjola et al., 2016)	≤ 25	PM_1 / $D_p \geq 2.5$	plume chasing	ELPI ^c	400 ± 280^b	
	(bus depot)			CPC		2.1 ± 0.1^b
EEV bus with SCR (Pirjola et al., 2016)	≤ 25	PM_1 / $D_p \geq 2.5$	plume chasing	ELPI ^c	280 ± 170^b	
	(bus depot)			CPC		7.0 ± 3.8^b
EEV with DOC+DPF+SCR (Rymaniak et al., 2017)	average at 45	PM_1 / 5.6-560	PEMS	MSS ^e	236^d	
				EEPS		0.02^d
EEV bus (Jarvinen et al., 2019)	stop and go	PM_1 / $D_p \geq 3$	plume chasing	ELPI ^c	200	
				CPC		8.6
Euro VI HDT in this study	29 ± 8^b	5.6-560	roadside	EEPS	5 ± 2	8.5 ± 4.6
Euro VI bus (Jarvinen et al., 2019)	stop and go	PM_1 / $D_p \geq 3$	plume chasing	ELPI ^c	70	
				CPC		5
Euro VI HDGV (Moody and Tate, 2017)	13-86	-	PEMS	-	$28-33^d$	-
Euro VI HDT (Grigoratos et al., 2019)	65-74	-	PEMS	-	-	$0.002-0.01^d$

HDT without available Euro type information	27±7 ^b	5.6-560	roadside	EEPS	47±23	7.5±7.3
Total Swedish HDT	28±7 ^b	5.6-560	roadside	EEPS	96±36	9.6±2.7
Total non-Swedish HDT	26±8 ^b	5.6-560	roadside	EEPS	117±42	11.1±4.2

Non-European HDV with different ATS

HDV with DPF (Wang et al., 2017; Quiros et al., 2016)	13-80	PM D _p ≥ 5	PEMS	gravimetric CPC	12-41 ^d	0.006-13.2
Heavy-duty HDV with DPF+SCR (Thiruvengadam et al., 2015)	driving cycle	PM	chassis dynamometer	gravimetric	6-29 ^d	-
HDV with DPF+SCR (Jiang et al., 2018)	driving cycle	PM _{2.5}	chassis dynamometer	gravimetric	3-97 ^d	-
HDT (model year 2004- 2006) (Preble et al., 2015)	accelerating or cruise at 48	D _p ≥ 2.5	roadside	CPC	-	47.2±9.7
HDT with SCR+DPF (model year 2010- 2013) (Preble et al., 2015)		D _p ≥ 2.5	roadside	CPC	-	15.9±11.5
HDV (mean model year 2005) (Bishop et al., 2015)	15.7-16.8	PM _{1.2}	OHMS ^g	digital mass monitor	650	-
HDV (mean model year 2009) (Bishop et al., 2015)	7.7-9.3	PM _{1.2}	OHMS ^g	digital mass monitor	31	-
HDV without after-treatment (Quiros et al., 2018)	driving cycle	PM _{2.5}	chassis dynamometer	gravimetric	1980 ^d	-
HDV+DPF (Quiros et al., 2018)	driving cycle	PM _{2.5}	chassis dynamometer	gravimetric	6-9 ^d	-

^a Given errors are at 95% CI.

^b Standard deviation.

^c ELPI, Electrical Low-Pressure Impactor.

^d Average fuel consumption of 0.26 L km⁻¹ for HDV during long haul and regional delivery tests (Rexeis et al., 2018), the density of 0.815 kg dm⁻³ (Swedish Environmental Protection Agency, 2013) of diesel particles were assumed for unit conversion.

^e MSS, Micro Soot Sensor.

^f SP-AMS, Soot Particle Aerosol Mass Spectrometer.

^g OHMS, On-Road Heavy-Duty Vehicle Emissions Monitoring System.

Table 2. Comparison of the average emission data^a for NO_x, NO₂/NO_x, CO and HC from the present study with literature data.

Vehicle type	Speed km h ⁻¹	Method	EF _{NOx} ^b g (kg fuel) ⁻¹	EF _{NO2} / EF _{NOx} ^b mass ratio %	EF _{CO} ^c g (kg fuel) ⁻¹	EF _{HC} ^c g (kg fuel) ⁻¹
Euro III HDT in this study	26±6 ^d	roadside	43.3±31.5	7.5±4.1	36.0±13.2	0.8±1.3
Euro III bus (Hallquist et al., 2013)	acceleration	roadside	16.1±9.7	-	16.1±16.1	<13
Euro III bus	≤25	plume chasing	12.7±1.8 ^d	-	-	-

(Pirjola et al., 2016)	(bus depot) ≤45 (bus line)	plume chasing	20.5	-	-	-
Euro III bus with DPF+SCR (Watne et al., 2018)	acceleration	roadside	-	-	13±10	0.02
Euro III HDV (Lau et al., 2015)	64 ± 13 ^d	plume chasing	-	24±4	-	-
Euro III & IV HDV (Kousoulidou et al., 2008)	-	model	-	14	-	-
Euro III HGV (Carslaw et al., 2011)	Average at 31	remote sensing	16.2±1.0 ^f	-	-	-
Euro III HGV (Carslaw and Rhys-Tyler, 2013)	28-60	remote sensing	-	24.1±4.7	-	-
Euro IV HDT in this study	23±8 ^d	roadside	19.8±10.1	2.7±2.9	22.1±10.3	0.7±1.1
Euro IV bus (Hallquist et al., 2013)	acceleration	roadside	12.9±6.5	-	16.1±16.1	<13
Euro IV bus with EGR+DPF (Pirjola et al., 2016)	≤25 (bus depot)	plume chasing	23.4±6.1 ^d	-	-	-
Euro IV bus with SCR (Watne et al., 2018)	roadside	acceleration	-	-	220-230	0.3-0.6
Euro IV HDV (Lau et al., 2015)	64 ± 13 ^d	plume chasing	-	28±5	-	-
Euro IV HGV (Carslaw et al., 2011)	average at 31	remote sensing	10.3±1.4 ^f	-	-	-
Euro IV HGV (Carslaw and Rhys-Tyler, 2013)	28-60	remote sensing	-	3.1±0.7	-	-
Euro V HDT in this study	27±7 ^d	roadside	22.2±3.8	6.0±2.8	22.8±5.1	0.9±0.4
Euro V bus (Hallquist et al., 2013)	acceleration	roadside	35.5±9.7	-	9.7±3.2	<13
Euro V bus with SCR (Liu et al., 2019)	stop and go (bus stop)	roadside	9.8±3.5 ^d	3.7±1.5 ^d	28 ^e	2.2 ^e
Euro V HDV (Lau et al., 2015)	64 ± 13 ^d	plume chasing	-	40±14	-	-
Euro V HDV (Kousoulidou et al., 2008)	-	model	-	18	-	-
Euro V HGV (Carslaw et al., 2011)	average at 31	remote sensing	13.3±5.8 ^f	-	-	-
Euro V HGV (Carslaw and Rhys-Tyler, 2013)	28-60	remote sensing	-	3.7±0.7	-	-
EEV HDT in this study	25±8 ^d	roadside	13.6±6.7	6.3±3.7	18.0±10.1	0.2±0.4
EEV bus with EGR +DPF (Pirjola et al., 2016)	≤25 (bus depot)	plume chasing	32.9±7.6 ^d	-	-	-
EEV bus with SCR (Pirjola et al., 2016)	≤25 (bus depot)	plume chasing	39.8±4.2 ^d	-	-	-
Euro VI HDT in this study	29±8 ^d	roadside	3.1±1.0	22.5±4.2	15.5±2.2	1.0±0.5
Euro VI HDT (Grigoratos et al., 2019)	65-74	PEMS	0.3-31.3	-	2.8-22.3	0.3-3.1
Euro VI HDV	-	model	-	35	-	-

(Kousoulidou et al., 2008)						
Euro VI HDV (Moody and Tate, 2017)	driving cycle	PEMS	2.2 ^f	-	-	-
HDT without available Euro type information	27±7 ^d	roadside	7.8±4.5	13.9±6.3	20.7±5.6	0.8±0.6
Total Swedish HDT	28±7 ^d	roadside	10.7±1.8	15.9±2.5	18.6±1.9	0.9±0.3
Total non-Swedish HDT	26±8 ^d	roadside	13.0±2.5	12.7±3.0	19.1±3.0	0.9±0.6

Non-European HDV with different ATS

Heavy-duty HDV with DPF+SCR (Thiruvengadam et al., 2015)	driving cycle	chassis dynamometer	3.8-27.8 ^f	-	0.1-13.4 ^f	<0.64 ^f
HDV with DPF+SCR (Jiang et al., 2018)	driving cycle	chassis dynamometer	0.2-66.4 ^f	-	0.006- 14.9 ^f	<1.3 ^f
HDV with DOC+DPF+SCR (Quiros et al., 2016)	12.7-85.6	mobile laboratory	1.7-11.8 ^f	-	0.9-2.8 ^f	0.1-0.4 ^f
HDV (May et al., 2014)	driving cycle	chassis dynamometer	30-43	-	-	-
HDV with SCR (May et al., 2014)	driving cycle	chassis dynamometer	11	-	-	-
HDV fleet average (Haugen et al., 2018)	22.5±0.9	remote sensing	12.4±0.6	8.9	5.9±0.9	2.2±0.4
HDT (model year 2004- 2006) (Preble et al., 2015)	accelerating or cruise at 48	roadside	16.5±1.7	3.4±1.8	-	-
HDT with SCR+DPF (model year 2010- 2013) (Preble et al., 2015)		roadside	5.1±1.2	22.1±8.4	-	-
HDT (model year 2001) (Burgard et al., 2006)	5-25	roadside	-	9.1±0.5	26.0±2.1	1.8±0.6
HDT (model year 2000) (Burgard et al., 2006)	20-40	roadside	-	6.1±0.1	37.9±1.6	3.3±0.4
Fleet average in 2006 (Bishop and Stedman, 2008)	28-36	roadside	2-5	-	17-24	1.9-2.3
HDT fleet average (Dallmann et al., 2012)	65	roadside	28±1.5	7.0	8.0±1.2	-
HDT (mean model year 2004) (Bishop et al., 2013)	22.2±0.4	remote sensing	20.6±0.6 ^d	9.7	8.2±0.6 ^d	3.7±0.1 ^d
HDT (mean model year 2009) (Bishop et al., 2013)	7.8±0.1	remote sensing	19.9±0.3 ^d	9.0	7.3±0.5 ^d	0.6±0.6 ^d

^a Given errors are at 95% CI.

^b In NO₂ equivalents.

^c RSD data. For the RSD data sets of multiple individuals, negative values were replaced by zero when calculating the averages.

^d Standard deviation.

^e Median.

^f Average fuel consumption of 0.26 L km⁻¹ for HDV during long haul and regional delivery tests (Rexeis et al., 2018), the density of 0.815 kg dm⁻³ (Swedish Environmental Protection Agency, 2013) of diesel particles were assumed.

6. Figure 2: For Euro III, it seems that the EF for black carbon is higher than for PM. How could this be?

Author Response: In the conversion of number concentrations to particle mass, particle sphericity and unit density were assumed. This might lead to an underestimation of PM. Nevertheless, we use this in the paper for easy comparison with the literature using similar experimental methodologies (Hallquist et al., 2013; Liu et al., 2019; Preble et al., 2015; Watne et al., 2018) in which unity density was used for the calculation of EF_{PM} .

In Fig. 2a, EF_{PM} includes both semi-volatile and non-volatile fractions. Using measurements with and without thermal desorption, we found that the ratio of $EF_{non-volatile\ PM}$ to EF_{PM} is generally higher for Euro III HDTs than other Euro type HDTs (Fig. R3). This explains why only Euro III HDTs show a higher EF_{BC} than EF_{PM} . In fact, there is a good linear relationship at EF_{PM} larger than $1\text{ mg (kg fuel)}^{-1}$ between the BC mass measured by the Aethalometer and the non-volatile particle mass measured at the outflow of a TD by the EEPS (Fig. S3). Compared to the EEPS, the detection limit of the Aethalometer is five times higher, which may influence the correlation between BC and PM at low mass loading conditions (when EF_{PM} is lower than $1\text{ mg (kg fuel)}^{-1}$).

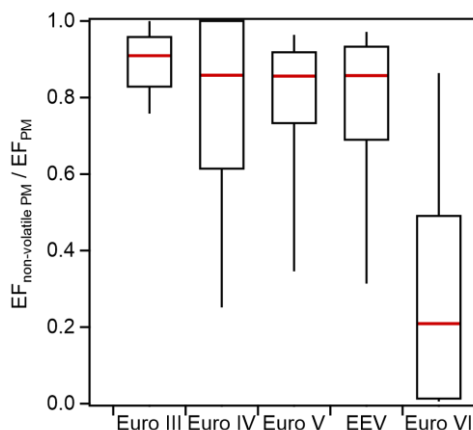


Figure R3. $EF_{non-volatile\ PM} / EF_{PM}$ for Euro III to Euro VI HDTs. Non-detectable pollutant emission signals for captured plumes have been replaced by EF_{min} . For box-and-whisker plots, the top and the bottom line of the box are 75th and 25th percentiles of the data, the red line inside the box is the median, and the top and bottom whiskers are 90th and 10th percentiles.

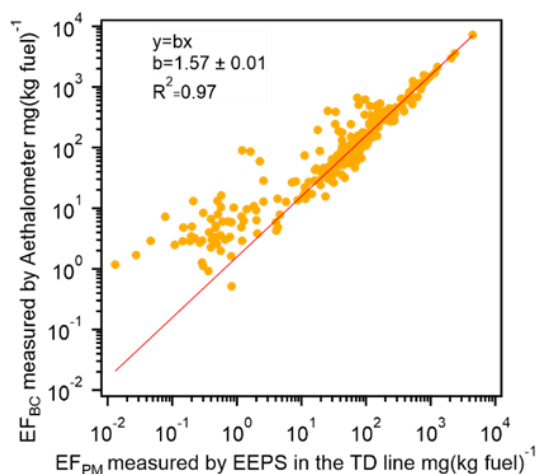


Fig. S3. Relationship between EF_{BC} measured by the Aethalometer and $EF_{\text{non-volatile PM}}$ measured by the EEPS in the TD line (unity density of particles was assumed).

7. Figure 4: This is very interesting. You might consider comparing these size resolved emission factors to previous studies that report similar EFs.

Author response and action: Thanks for your suggestion, we have added the following discussion in red and Fig. 4f to the manuscript (line 355 in the revised manuscript and line 363 in the marked-up manuscript):

The EF_{PN} of the accumulation mode particles shows a decreasing trend from Euro III to EEV HDTs. The accumulation mode of the Euro VI HDTs was insignificant. For heavy-duty diesel engines without a particulate filter, nucleation mode particles are mainly formed from organics. For vehicles with DPF both organics and the fuel sulphur content might influence the formation of nucleation mode particles (Vaaraslahti et al., 2004). Thiruvengadam et al. (2012) found a direct relationship between exhaust nanoparticles in the nucleation mode and the exhaust temperature of the DPF-SCR equipped diesel engine. These factors lead to high variability in the nucleation mode fraction of EF_{PN} . Figure 4f shows that HDVs with DPF (dashed lines) exhibited lower emissions of accumulation mode particles, with no significant reduction in nucleation mode particles when compared to HDVs without DPF (solid lines). In general, the absence of significant accumulation mode particles from Euro VI HDTs was consistent with observations made from DPF equipped HDVs. High emissions of accumulation mode particles from Euro III HDTs were consistent with measurements from HDVs without DPF in previous studies (Liu et al., 2019; Hallquist et al., 2009; Preble et al., 2015).

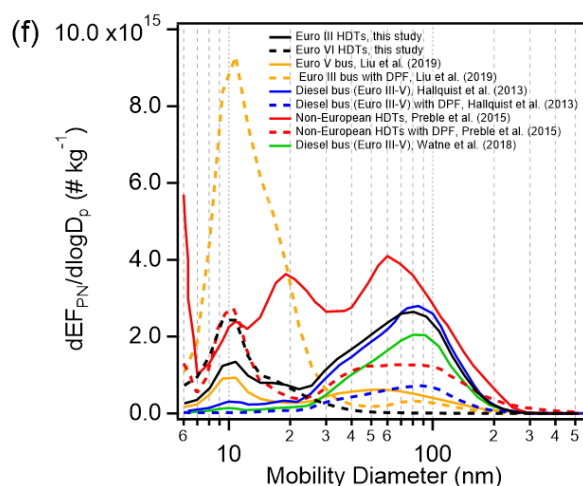


Figure 4f. Comparisons of mean size-resolved EF_{PN} of HDVs in this study and previous studies.

Reference

Dallmann, T. R., Harley, R. A., and Kirchstetter, T. W.: Effects of diesel particle filter retrofits and accelerated fleet turnover on drayage truck emissions at the Port of Oakland, *Environ Sci Technol*, 45, 10773-10779, <https://doi.org/10.1021/es202609q>, 2011.

Hallquist, A. M., Jerksjö, M., Fallgren, H., Westerlund, J., and Sjödin, A.: Particle and gaseous emissions from individual diesel and CNG buses, *Atmospheric Chemistry and Physics*, 13, 5337-5350, <https://doi.org/10.5194/acp-13-5337-2013>, 2013.

Liu, Q., Hallquist, Å. M., Fallgren, H., Jerksjö, M., Jutterström, S., Salberg, H., Hallquist, M., Le Breton, M., Pei, X., and Pathak, R. K.: Roadside assessment of a modern city bus fleet: Gaseous and particle emissions, *Atmospheric Environment: X*, 100044, <https://doi.org/10.1016/j.aeaoa.2019.100044>, 2019.

Ntziachristos, L., Giechaskiel, B., Pistikopoulos, P., Samaras, Z., Mathis, U., Mohr, M., Ristimäki, J., Keskinen, J., Mikkanen, P., and Casati, R.: Performance evaluation of a novel sampling and measurement system for exhaust particle characterization, 10.4271/2004-01-1439, 2004.

Preble, C. V., Dallmann, T. R., Kreisberg, N. M., Hering, S. V., Harley, R. A., and Kirchstetter, T. W.: Effects of Particle Filters and Selective Catalytic Reduction on Heavy-Duty Diesel Drayage Truck Emissions at the Port of Oakland, *Environ Sci Technol*, 49, 8864-8871, <https://doi.org/10.1021/acs.est.5b01117>, 2015.

Watne, A. K., Psichoudaki, M., Ljungstrom, E., Le Breton, M., Hallquist, M., Jerksjö, M., Fallgren, H., Jutterstrom, S., and Hallquist, A. M.: Fresh and Oxidized Emissions from In-Use Transit Buses Running on Diesel, Biodiesel, and CNG, *Environ Sci Technol*, 52, 7720-7728, <https://doi.org/10.1021/acs.est.8b01394>, 2018.

A transition in atmospheric emissions of particles and gases from on-road heavy-duty trucks

Liyuan Zhou¹, Åsa M. Hallquist^{2*}, Mattias Hallquist³, Christian M. Salvador³, Samuel M. Gaita³, Åke Sjödin², Martin Jerksjö², Håkan Salberg², Ingvar Wängberg², Johan Mellqvist⁴, Qianyun Liu¹, Berto P. Lee¹, Chak K. Chan^{1*}

¹School of Energy and Environment, City University of Hong Kong, Hong Kong, China

²IVL Swedish Environmental Research Institute, Gothenburg, Sweden

³Department of Chemistry and Molecular Biology, University of Gothenburg, Gothenburg, Sweden

⁴Earth and Space Sciences, Chalmers University of Technology, Gothenburg, Sweden

Correspondence to: Åsa M. Hallquist (asa.hallquist@ivl.se), Chak K. Chan (Chak.K.Chan@cityu.edu.hk)

Abstract. The transition in extent and characteristics of atmospheric emissions caused by the modernisation of the heavy-duty on-road fleet were studied utilising roadside measurements. Emissions of particle number (PN), particle mass (PM), black carbon (BC), nitrogen oxides (NO_x), carbon monoxide (CO), hydrocarbon (HC), particle size distributions and particle volatility were measured from 556 individual heavy-duty trucks (HDTs). Substantial reductions in PM, BC, NO_x, CO and to a lesser extent PN were observed from Euro III to Euro VI HDTs by 99%, 98%, 93% and 57% for the average emissions factors of PM, BC, NO_x, and CO respectively. Despite significant total reductions in NO_x emissions, the fraction of NO₂ in the NO_x emissions increased continuously from Euro IV to Euro VI HDTs. Larger data scattering was evident for PN emissions in comparison to solid particle number (SPN) for Euro VI HDTs, indicating a highly variable fraction of volatile particle components. Particle size distributions of Euro III to EEV HDTs were bimodal, whereas those of Euro VI HDTs were nucleation mode dominated. High emitters disproportionately contributed to a large fraction of the total emissions with the highest-emitting 10% of HDTs in each pollutant category being responsible for 65% of total PM, 70% of total PN and 44% of total NO_x emissions, respectively. Euro VI HDTs, which accounted for 53% of total kilometres driven by Swedish HDTs, were estimated to only contribute to 2%, 6%, 12% and 47% of PM, BC, NO_x, and PN emissions. A shift to a Euro VI HDTs dominant fleet would promote a transition of atmospheric emissions towards low PM, BC, NO_x, and CO levels. Nonetheless, reducing PN, SPN, and NO₂ emissions from Euro VI HDTs is still important to improve air quality in urban environments.

1 Introduction

Vehicular emissions contribute significantly to gaseous and particle pollutants in the urban atmosphere and description of their extent and characteristics are key input components for urban air quality modelling. As technology and traffic demands change, so do the characteristics of the emissions. In Europe, the introduction of new legislation, especially Euro VI, has aimed to reduce emissions of many pollutants. Legislation exists for particles (mass and number) and selected gases, however, there are

also many components of the emissions that are not directly regulated but are potentially detrimental to human health. The most notable example of a non-regulated pollutant is the abundance of ultrafine particles (UFP) (Campagnolo et al., 2019), defined as particles with a diameter less than 100 nm (Zhu et al., 2002). UFPs can cause lung disease, an increase of blood coagulability and cardiovascular disease and related mortality (Du et al., 2016). In the most recent Euro class, this has partly been covered by introducing a limit on the solid particle number (SPN) while volatile particles and particles less than 23 nm are not considered. Furthermore, the legislation has mainly been based on test cycles performed before introducing a new engine into the market but only recently also off-cycle and in-service conformity testing has been introduced, hence the actual performance in real-traffic is less constrained, where driving pattern, maintenance, and age of engine will vary. Here real-traffic studies may capture variability between vehicles and also put the effect of new legislation and parallel phase-out of older technology into perspective for the abatement of urban air pollution.

Heavy-duty vehicles (HDVs) usually account for a smaller number fraction of on-road vehicles than light-duty vehicles but they tend to contribute to a disproportionately high fraction of mobile source particulate matter emissions (Gertler, 2005; Cui et al., 2017). Emissions from HDVs, often diesel, are significantly affected by the engine type, exhaust after-treatment system (ATS), and driving conditions. The main purpose of ATS is the reduction of particulate and gaseous pollutants. Diesel Oxidation Catalysts (DOC) are used for reducing hydrocarbon emissions, selective catalytic reduction (SCR) systems or exhaust gas recirculation (EGR) are employed to mitigate NO_x emissions, and diesel particulate filters (DPF) can reduce particulate matter mass emissions. The use of ATS can, however, bring undesired side effects. For example, conversion of SO₂ to SO₃ and increased gaseous sulfuric acid formation have been reported from DOCs (Arnold et al., 2012). DPFs potentially enhance the formation of UFP (Herner et al., 2011; Preble et al., 2017). Retrofitted DPF can slightly reduce the NO_x emissions but significantly increase the direct emission of NO₂ by as much as a factor of 8 (Smith et al., 2019). Failure of the temperature-dependent SCR in eliminating the excess NO₂ leads to an elevated NO₂ to NO_x ratio (Herner et al., 2009; Bishop et al., 2010; He et al., 2015).

The Euro standard regulates vehicle emission limits in Europe. The Euro III standard was established in 1999, and more stringent Euro IV and Euro V standards were implemented in 2005 and 2008, respectively. The Enhanced Environmentally Friendly Vehicle (EEV) is a voluntary environmental standard which lies between the levels of Euro V and Euro VI. The currently enforced Euro VI standard has been implemented since 2013-2014 and introduced SPN limits into the regulation for the first time. Generally, newer engines are expected to perform better in controlling pollutant emissions. Guo et al. (2014) reported that Euro V diesel buses performed better than Euro IV and Euro III diesel buses in the emissions of all the pollutants, except for the generation of more nucleation mode particles. The latest 2018 European Environmental Agency (EEA) report confirms an overall improvement in the European air quality, while the road transport sector remains one of the major contributors to pollutant emissions and the largest contributor to the total NO_x emission (Grigoratos et al., 2019; EEA, 2018). A recent on-board sensor-based study pointed out that HDVs emitted more than three times the NO_x certification standard during real-world hot-driving and idling operations (Tan et al., 2019). Published data regarding particle and gaseous pollutant emissions from real-world on-road Euro VI heavy-duty vehicles are scarce and often limited by the small sample

size (Giechaskiel et al., 2018; Grigoratos et al., 2019; Moody and Tate, 2017). Remote sensing sampling can measure a large sample size of vehicles but are usually restricted to gaseous pollutant emissions (Burgard and Provinsal, 2009; Burgard et al., 2006; Carslaw et al., 2011). From an air quality perspective, the particle emissions are crucial. The complexity and dynamics of atmospheric particles require detailed information of its emission for atmospheric modelling and for descriptions of their health impacts. For example, particle size is important to determine the effects on respiratory deposition in humans (Manigrasso et al., 2017; Lv et al., 2016).

Diesel exhaust particles are a complex mixture of numerous semi-volatile and non-volatile species, and the semi-volatile compounds will experience gas-to-particle partitioning in the atmosphere (Robinson et al., 2007; Donahue et al., 2006). Biswas et al. (2009) reported that the semi-volatile fraction in HDV emission is more oxidative than the refractory particles, which may change the redox state in cells and cause oxidative stress. Semi-volatile organic compounds, such as PAHs and their derivatives may possess genotoxic and carcinogenic characteristics (Bocchi et al., 2016; Vojtisek-Lom et al., 2015). Giechaskiel et al. (2009) suggested using the volatile mass fraction as a metric to assess health effects as the volatile mass dissolves in the lung fluid and thereby interacts with epithelial cells. Deploying a Volatility Tandem Differential Mobility Analyzer in suburban Guangzhou, China, Cheung et al. (2016) found that 57–71 % of ambient particles between 40 and 300 nm contain volatile components. Furthermore, the evaporated semi-volatile compounds from the particle phase can be further oxidized to form secondary organic aerosols (SOA) (Hallquist et al., 2009; Gentner et al., 2017). To better quantify the health effects and global and regional contributions of road traffic to the total particle burden in the atmosphere, information on the volatility properties of vehicle particulate emissions is needed.

Different approaches have been applied to study the emissions from HDTs (Franco et al., 2013). Chassis dynamometer tests provide relatively comprehensive emission characteristics of individual vehicles (Jiang et al., 2018; Chen et al., 2018; Thiruvengadam et al., 2015), but the artificial driving cycles make it difficult to simulate the full range of real-world driving conditions. Portable emission measurement systems (PEMS) (Grigoratos et al., 2019; Pirjola et al., 2017) and plume chasing studies (Lau et al., 2015; Pirjola et al., 2016) have been conducted in real-world environments but are often limited by small sample sizes. Tunnel studies (Li et al., 2018) measure the average emission of all vehicles passing through the tunnel without specific emission information of vehicle types. Roadside measurements, as presented in this study, provide an opportunity to study real-world on-road traffic emissions on large sample sizes with individual vehicle information (e.g. Hallquist et al., 2013; Dallmann et al., 2012; Carslaw and Rhys-Tyler, 2013; Watne et al., 2018).

In this work, we measured the gaseous and particle emissions from 556 on-road individual HDTs and quantified changes in emissions and the potential transition in characteristics caused by the reduction achieved by the introduction of more stringent Euro standards. Particle size distributions and particle volatilities were investigated with respect to Euro class, and pollutant emission characteristics were studied with respect to year of registration. Cumulative pollutant distributions were established to demonstrate the importance of controlling high-emitters in reducing total emissions. The typical contribution of air pollution emissions from each Euro class HDTs was estimated based on total vehicle kilometres driven. Results of the presented pollutant emission factors in our study will be useful for both emission models and emission inventories. A clear

99 transition of atmospheric pollutant emission trends was evident and can provide useful guidance for policies regarding the
100 regulation of existing fleets.

101 **2 Methods**

102 **2.1 Field sampling site**

103 Pollutant emissions from HDTs were measured at a roadside location in Gothenburg, Sweden (Fig. 1). The HDTs passed the
104 sampling location with an average speed of 27 km h⁻¹ and acceleration of 0.7 km h⁻¹ s⁻¹ on a slight uphill slope (~2°). Under
105 such uphill driving conditions, vehicles are expected to emit higher levels of pollutants than during downhill and cruise driving.
106 This will be further examined in Sect. 3.3.

107 **2.2 Air sampling**

108 The sampling of the emissions was conducted in line with Hallquist et al. (2013), i.e. extractive sampling of passing HDT
109 plumes. Air was continuously drawn through a flexible copper tube to the instruments inside a container. A similar
110 experimental set-up was previously applied to on-road bus emission measurements (Liu et al., 2019). Particles were measured
111 by an EEPS (Engine Exhaust Particle Sizer, Model 3090 TSI Inc.) in the size range of 5.6-560 nm with high time resolution
112 (10 Hz) while total particle number was measured by a butanol-based condensation particle counter (CPC Model 3775 TSI
113 Inc., 50 cut-off diameter 4 nm). Particle numbers measured by the two instruments showed a good correlation ($R^2=0.73$)
114 (Fig. S1). A second EEPS measured the outflow of a TD (thermodenuder, Dekati, Inc.), enabling estimations of particle
115 volatility. The data were corrected for size-dependent losses in the TD. The temperature inside the TD heating zone was set to
116 250°C with a residence time of ~ 0.6 s, which is generally sufficient to evaporate nearly all the organics and sulphates from
117 the particles (Huffman et al., 2008). However, organics with extremely low volatility (organic saturation mass concentration,
118 $C^* < 10^{-5} \mu\text{g m}^{-3}$ at 298 K) may still be retained even at this high temperature (Gkatzelis et al., 2016). Thus, in this study, we
119 define the ‘non-volatile components’ as particle components that remain after passing through the TD operating at 250°C.
120 Differences in counting efficiencies between the two EEPS were accounted for by size-dependent correction factors (typically
121 less than 10%), which were retrieved by simultaneous sampling of ammonium sulphate particles by both EEPS and direct
122 comparison of their measured size distributions (Fig. S2). BC and the mixture of BC and brown carbon (BrC) were measured
123 by an Aethalometer at 880 nm and 370 nm respectively (Model AE 33, Magee Scientific Inc.). The determination of particle
124 mass concentrations by the integrated particle size distribution (IPSD) method requires information on particle density. Particle
125 sphericity and unit density were assumed due to a lack of detailed knowledge about the chemical composition of the emitted
126 particles. Figure S3 shows that there is a good linear relationship at EF_{PM} larger than 1 mg (kg fuel)⁻¹ between the BC mass
127 measured by the Aethalometer and the non-volatile particle mass measured by the EEPS but assuming sphericity and unit
128 density the EEPS mass is lower, which indicates a potential underestimation of the effective non-volatile particle density.

Compared to the EEPS, the detection limit of the Aethalometer is five times higher, which may influence the correlation between BC and PM at low mass loading conditions (Fig. S3). There have been several studies on the morphology and density of combustion generated particles and its detailed dependence on combustion and dilution condition (e.g. Maricq and Ning, 2004; Ristimäki et al., 2007; Liu et al., 2009; Zheng et al., 2011; Quiros et al., 2015). However, to be consistent, avoid assumptions and to compare with a majority of previously reported data, unity density was used for further discussion and comparisons. CO₂ was measured by a non-dispersive infrared gas analyser (LI-840, LI-COR Inc.). NO_x and NO were measured simultaneously by two separate chemiluminescent analysers (Model 42i, Thermo Scientific Inc.), and the NO₂ concentration was calculated from the difference between the NO_x and NO concentrations. SO₂ was measured by a pulsed fluorescence gas analyser (Model 43c, Thermo Scientific Inc.). A Remote Sensing Device (RSD) (OPUS Inspection Inc.) was used to measure the gaseous emission factors of CO, NO_x, and HC. Briefly, the instrument was set up with a transmitter and a receiver on the same side of the truck passing lane and a reflector on the opposite side. Co-linear beams of IR and UV light are emitted and cross-reflected through the plume and light attenuation related to respective pollutant concentrations are measured. Gas pollutant concentrations were determined relative to CO₂ as measured by the RSD. NO_x and NO measured by the gas analysers and the RSD were in agreement ($R^2=0.53$ and 0.66 respectively, Figs. S4, S8a). The High-Resolution Time-of-Flight Chemical Ionization Mass Spectrometer (HR-ToF-CIMS) shown in Fig. 1 was used to characterise the chemical composition of organic and inorganic compounds in the gas and particle phase, emitted from the HDTs. However, the extensive chemical characterisation is beyond the scope of this work and will be presented elsewhere.

A schematic of the experimental setup is given in Fig. 1 along with some examples of typical temporal profiles of pollutant concentrations in the plumes from Euro III and Euro VI HDTs. A camera at the roadside recorded the HDT plate numbers, which was used for identification and to obtain engine Euro type information. ~~All the instruments were operated at least at 1Hz of sampling frequency to capture rapidly changing concentrations during the passage of a HDT.~~ All the instruments were at least operated at 1Hz of sampling frequency to capture rapidly changing concentrations during the passage of a HDT, which is sufficiently fast to measure pollutant concentration peaks (typically 5 to 20 s in duration) as shown in Fig. 1c-e. In general, the duration of a peak was around 5s, for NO_x slightly longer, limiting measurements of high-frequency passages. Euro III HDTs typically emitted a significant amount of PN, PM, NO_x, and non-volatile components (Fig. 1c). More than 95% of Euro III, Euro IV, Euro V, and EEV HDTs had measurable particle emission signals. Significant differences in low particle and gaseous emissions were evident for Euro VI HDTs (Fig. 1d and e).

2.3 Data analysis

The exact time of individual HDTs passing the sampling inlet was determined from the camera recordings and the associated plume pollutant concentrations were integrated to calculate corresponding pollutant emission factors of individual HDTs as described by Hallquist et al. (2013). Emissions of gases and particles from individual HDTs were normalized by the CO₂ concentration to compensate for different degrees of dilution during sampling (Janhäll and Hallquist (2005)). CO₂ peak concentrations exceeding four times the standard deviation of the background signal were used as the base criterion for

successful plume capture. Peaks in NO_x, PN, PM, and BC concentrations concurrent with that of CO₂ signify the presence of co-emitted pollutants in a HDT plume. Emission factors (EFs) of gaseous and particle emissions for individual HDTs can then be expressed in units of amount of pollutant emitted per kg fuel burned based on the carbon balance method (Ban-Weiss et al., 2009; Hak et al., 2009):

$$EF_{pollutant} = \frac{\int_{t_1}^{t_2} ([pollutant]_t - [pollutant]_{t_1}) dt}{\int_{t_1}^{t_2} ([CO_2]_t - [CO_2]_{t_1}) dt} \times EF_{CO_2}, \quad (1)$$

where $EF_{pollutant}$ is the emission factor of the respective pollutant. The time interval of t_1 to t_2 represents the period when the instruments measured the concentration of an entire pollutant peak from an individual HDT (see Fig. 1c-e). [Dallmann et al. \(2011\)](#) and [Preble et al. \(2015\)](#) used the concepts of inflection points to identify t_1 and t_2 . In our study, t_1 and t_2 were determined similarly: t_1 is the point before the pollutant concentration intensity increases abruptly and t_2 is when the intensity becomes relatively flat and undistinguishable compared to background levels. It is noted that the integrated peak intensity is insensitive to the exact location of t_2 since the added integrated signals at or beyond this point are fluctuating around zero. t_1 and t_2 were determined independently of each pollutant peak to account for differences in the time response of individual instruments to the exhaust plume. $\int_{t_1}^{t_2} ([pollutant]_t - [pollutant]_{t_1}) dt$ and $\int_{t_1}^{t_2} ([CO_2]_t - [CO_2]_{t_1}) dt$ are the changes in concentration of a pollutant and CO₂ during this time interval. EF_{CO_2} of 3158 g (kg diesel fuel)⁻¹ was used as the emission factor of CO₂, assuming complete combustion and a carbon content of 86.1% as given in [Edwards et al. \(2014\)](#). Emission factors for plumes with pollutant concentrations lower than our set detection limit (four times the standard deviation of the pollutant background signal) were replaced by the minimum value among all recorded emission factors (EF_{min}) rather than being omitted to avoid inflating emissions from low-emitting HDTs.

3 Results and Discussion

3.1 Fleet compositions

A total of 675 resolved plumes from 556 individual HDTs for the carriage of goods with weights exceeding 12 tonnes were identified. There were 330 Swedish HDTs with Euro type information, 46 Swedish HDTs from which Euro type information was not available, and 180 foreign licensed non-Swedish HDTs. Among the 330 Swedish trucks, Euro III, Euro IV, Euro V, EEV, and Euro VI HDTs accounted for 3%, 5%, 30%, 5%, and 57%, respectively (Fig. S5).

3.2 Emissions variability

Differences in operating and ambient conditions may lead to differences in pollutant emission factors for the same HDT. In this study, we utilized measurement data from 55 HDTs which passed the sampling location repeatedly, yielding a total of 137 plumes. The average pollutant emission factors of each HDT plotted against the individual plume measurements of the corresponding HDT are shown in Fig. S6. In general, the emission factors of PM, non-volatile PN, and NO_x showed little

variation ($R^2 \geq 0.77$) among multiple passages of the same HDT, however, higher variability was observed in the PN emissions. This is likely related to variations in the formation of nucleation mode particles from volatile compounds which is more sensitive to driving (Zheng et al., 2014) and dilution conditions. In the following discussion, for HDTs with multiple passages, the average pollutant emission factors of all the detected plumes were used for that individual HDT.

3.3 Emissions factors (EFs) of particles and gaseous pollutants

Figure 2 a and b show the box-and-whisker plots of PM and PN emission factors (EFs) for different Euro classes. Generally, both PM and PN emissions decreased with more stringent Euro emission standards, and especially for Euro VI where larger changes in emission characteristics were evident. These decreasing trends are statistically significant at the 95% CI using the Jonckheere-Terpstra test, a nonparametric test for trends in ordered groups. In addition to PM and PN, the emission trends of BC, NO_x, CO and HC with respect to the level of stringency of Euro standards were statistically examined. Using Euro III HDTs (median $EF_{PM} = 586 \text{ mg (kg fuel)}^{-1}$) as a baseline, the median EF_{PM} for Euro IV, Euro V, EEV, and Euro VI HDTs have been reduced by 78.1%, 86.1%, 88.9%, and 99.8% respectively. In particular, Euro VI HDTs has a median EF_{PM} of only $1.4 \text{ mg (kg fuel)}^{-1}$ (Fig. 2a). While it is noted that Euro III to Euro VI standard certifications are based on chassis dynamometer cycle measurements, the Euro VI regulations have started to include additional off-cycle and in-service conformity testing. The Euro emission standard of transient testing for heavy-duty engines gives emission limits as brake specific emission factors, as mass (g) or number (#) of a specific pollutant per kWh. In order to enable a comparison with the Euro emission standard, the EFs in g (or #) per kg fuel were converted using a brake specific fuel consumption (BSFC) of 231.5 g kWh^{-1} . This is the average value for the long haul and regional delivery cycles of chassis dynamometer tests of a typical rigid Euro VI truck (Rexeis et al., 2018). The uncertainty of the BSFC for different Euro class HDTs operating over a wide range of engine conditions is generally within 25% (Mahmoudzadeh Andwari et al., 2017; He et al., 2017; Dreher and Harley, 1998; Heywood, 1988). Note that our measurements represent points of time similar to those in a cycle where the particle emissions can be most prominent. Looking at a whole cycle, this value will be averaged, hence the results from our instantaneous plume measurements may represent an upper limit of the emissions. In Fig. 2a, the right y-axis gives the EFs converted into units of g kWh^{-1} and the Euro standards are shown as blue crosses.

In general, the measured median EF_{PM} are lower than the Euro standards for all HDT types. In particular, the median EF_{PM} for Euro VI HDTs is more than one order of magnitude lower than the Euro standard regulation value since Diesel Particulate Filters (DPFs) are required for these Euro VI HDTs to comply with PM and PN standards (Williams and Minjares, 2016). No information about potential retrofits of tested HDTs was available for the vehicles measured in this study. The effectiveness of DPF in reducing particle emissions have been confirmed by various studies (Martinet et al., 2017; May et al., 2014; Mendoza-Villafuerte et al., 2017; Moody and Tate, 2017; Preble et al., 2015). For example, Bergmann et al. (2009) illustrated that post-DPF PM concentrations decreased by 99.5% compared with pre-DPF for the New European Driving Cycle (NEDC). In real-world measurements, at least ~90% reductions in PM emissions compared to typical pre-DPF levels have been reported (Bishop et al., 2015). Euro emission standards for PM of Euro IV and Euro V heavy-duty diesel engine are the

same, while the measured median EF_{PM} of the Euro V fleet was around 1.5 times lower than that of the Euro IV fleet. The control of diesel engine emissions typically requires a compromise between NO_x and particle emission reduction (Clark et al., 1999). The NO_x emission standard is more stringent for Euro V compared to Euro IV (a factor of 43% lower), and hence Euro V HDTs are generally equipped with SCR or EGR to reduce NO_x . In contrast, Euro IV engines are rarely equipped with NO_x after-treatment systems and thus must achieve the NO_x emission limits by tuning the engine performance parameters at the expense of higher PM emissions (Preble et al., 2018; Van Setten et al., 2001). In each of the Euro III, Euro IV, Euro V, and EEV classes, 25-50% of all the measured HDTs had an EF_{PM} higher than their corresponding Euro standards. As described previously, this comparison with the Euro standard is relative and indicative. The higher emissions from individual HDTs may indicate deterioration of engine performance due to wear caused by aging, mileage accumulation, or inadequate maintenance. Our study shows that Euro VI HDTs generally have low PM emissions, but HDTs from older Euro classes frequently exceeded their PM emission limits, suggesting that improved maintenance and suitable retrofitting of older engines are needed.

For PN emissions, EF_{PN} shows an overall trend similar to EF_{PM} . However, large data scatter was evident for Euro VI HDTs, likely due to the sensitivity of nucleation mode particle formation to changes in driving conditions (Fig. 2b). Zheng et al. (2014) reported high concentrations of nucleation mode particles under uphill driving conditions but low concentrations under cruise and downhill driving conditions. It is important to note that the median EF_{PN} of Euro VI HDTs was significantly lower than those from the other Euro type HDTs, which indicates efficient PM removal by the DPF without compromising on total PN emission. Nonetheless, the decrease of particle number in the accumulation mode removes particle surface area available for condensation and therefore favours nucleation of organics from fuel and lubrication oil. Le Breton et al. (2019) confirmed the contribution of lubrication oil in bus emissions. Besides, DPFs can act as a sulphur reservoir and when excess sulphur is released, SO_2 to SO_3 conversion can take place once the after-treatment temperature reaches a critical level (Herner et al., 2011). In this case, total particle number emissions can increase due to nucleation from gas-phase sulphuric acid. Since the fuel sulphur content is low, more than 90% of Euro VI HDTs had an EF_{SO_2} lower than the threshold in this study, organics would play a more important role in the formation of nucleation mode particles.

Figure 2c shows that the median EF_{BC} was reduced by more than 99% for Euro VI HDTs compared to Euro III HDTs, and the median EF_{BC} of Euro VI HDTs was even at the threshold ($0.2\text{mg (kg fuel)}^{-1}$). ~~The BC emissions generally showed an overall decrease when moving towards newer Euro classes, which is similar to the EF_{PM} trend with the exception of Euro IV HDTs. The BC emissions generally showed a decrease from Euro III to Euro VI HDTs (Jonckheere-Terpstra test, $p<0.01$), which is similar to the EF_{PM} trend with the exception of Euro IV HDTs.~~ Compared with Euro V HDTs, the median EF_{BC} of Euro IV HDTs is 35% lower, however, the emission of the mixture of BC and BrC from Euro IV HDTs is higher (Fig. S7a). Euro IV HDTs had the highest BrC contribution to the total light-absorbing substances among all the Euro classes (Fig. S7b).

Figure 2d compares the emissions of NO_2 and NO_x from different Euro class HDTs. The vertical lines represent the different Euro standards. HDTs with either EF_{NO_2} or EF_{NO_x} lower than the detection limits of the instruments were removed in Fig. 2d for illustration purposes, while all the presented statistical analyse include all the data as outlined above. In general, Euro VI HDTs exhibit more than 90% reduction in both median and average EF_{NO_x} compared to Euro III HDTs. This is

258 consistent with Carslaw et al. (2011) who estimated a 93% NO_x reduction from Euro III to Euro VI for heavy goods vehicles
 259 (HGV) in the United Kingdom. Relatively, the Euro V HDTs had a larger fraction exceeding its Euro standard, which may be
 260 due to the combined effects of poor engine tuning and the inactivity (low temperature) or deterioration of SCR systems. Newer
 261 engines tend to exhibit a higher NO₂ emission fraction at a similar NO_x level, and the Euro VI HDTs show a relatively low
 262 median EF_{NO2} with a large range of data scatter and several high emitters. A continuous increase of EF_{NO2}/EF_{NOx} was evident
 263 from Euro IV to Euro VI HDTs (Fig. S8b). This trend is consistent with Kozawa et al. (2014), who reported an increase in the
 264 share of NO₂ to total NO_x from Euro III to Euro V vehicles. Euro VI HDTs have a higher NO₂ fraction because the DOC
 265 upstream of the filter is used to convert NO to NO₂ to control the soot loading in the DPF and facilitate the passive
 266 regeneration (Van Setten et al., 2001). A failure of the NO₂ reduction due to the inactivity of the SCR, resulting from low
 267 exhaust gas temperature, may result in a higher NO₂ emission (Bishop et al., 2010; Heeb et al., 2010; Herner et al., 2009; May
 268 et al., 2014; Thiruvengadam et al., 2015). A more significant decrease in NO_x than NO₂ emissions of Euro VI HDTs may cause
 269 an increase of EF_{NO2}/EF_{NOx}.

270 Table 1 compares the average emission data of PM and PN of the current work with previous studies according to the
 271 HDT type and gives information on used measurement methods and driving conditions. Generally, the EF_{PM} and EF_{PN} in this
 272 study are within the reported ranges of HDV emissions in the literature. Our estimated EF_{PM} of Euro III HDTs are comparable
 273 to those of Euro III buses in Hallquist et al. (2013) and Pirjola et al. (2016). HDTs and buses within the same Euro class emit
 274 similar amounts of PM. Watne et al. (2018) show that DPF retrofitted Euro III buses have much lower particle EFs. While
 275 EF_{PM} is highly dependent on driving conditions such as speed and acceleration, the average EF_{PM} of Euro IV, Euro V and EEV
 276 HDTs of this study: 172, 146, and 78 mg (kg fuel)⁻¹, respectively, are comparable to trends in previous studies (Hallquist et al.,
 277 2013; Pirjola et al., 2016; Watne et al., 2018). Average EF_{PM} of Euro VI HDTs (5 mg (kg fuel)⁻¹/ 1.1 mg km⁻¹) is within the
 278 range of emissions from HDVs with DPFs, e.g., 0.6 - 20.5 mg km⁻¹ for a recent chassis dynamometer test (Jiang et al., 2018)
 279 and 2.5 - 8.7 mg km⁻¹ for road measurements in California (Quiros et al., 2016). Note that size ranges and measurement
 280 methodologies may differ among the studies as listed in Table 1. Since most of the particle emissions related to road traffic
 281 combustion are below 560 nm (Fig. 4), the size range in our study is comparable to most other wider range PM measurements.
 282 Larger particles from road measurements of total PM may include non-combustion-related particles, e.g. resuspended road
 283 dust, tire and brake particles, and should be interpreted with caution. In contrast to EF_{PM}, a much less obvious decrease in
 284 average EF_{PN} was observed across different Euro classes. The reason for the high average particle emission for EEV and Euro
 285 VI is likely due to high emissions of nucleation mode particles from a number of HDTs.

286 In Figure 3a, EF_{PM} and EF_{PN} of individual HDTs in this study and selected previous studies are plotted. HDTs with either
 287 EF_{PM} or EF_{PN} lower than the detection limits of the instruments (0.07 mg (kg fuel)⁻¹ and 2.8×10¹¹# (kg fuel)⁻¹ respectively)
 288 were removed from the figure (24% of the data) for illustration purposes, while all the presented statistical analyses include all
 289 the data as outlined above. Generally, both EF_{PM} and EF_{PN} exhibited a decreasing trend from Euro III to Euro IV and from
 290 Euro V to EEV HDTs. Generally, both EF_{PM} and EF_{PN} exhibited a decreasing trend from Euro III to Euro IV and from Euro
 291 V to EEV HDTs (Jonckheere-Terpstra test, p<0.01). Overall, Euro VI HDTs had drastically lower PM emissions but highly

scattered PN emissions. Older Euro type buses retrofitted with DPF were shown to have reduced particle emissions, and some retrofitted Euro III buses (black open triangles in Fig. 3a) may perform as well as Euro VI HDTs, indicating the effectiveness of retrofitting older HDTs.

In more recent Euro standards, PN regulation has been introduced. The SPN as defined by the European Particle Measurement Program (PMP) is the number of particles which remain after passing through an evaporation tube with a wall temperature of 300-400°C (Zheng et al., 2011). The PMP only measures and regulates solid particles with a diameter larger than 23 nm because measurements of smaller particles in the nucleation mode have poor repeatability (Martini et al., 2009). SPN larger than 23 nm was integrated into the European emission regulation in 2013 for Euro VI heavy-duty engines (Giechaskiel et al., 2012). A potential issue of evaporation measurements is that a fraction of the sub-23 nm particles can also be formed downstream of the European PMP methodology through re-nucleation of semi-volatile precursors (Zheng et al., 2012; Zheng et al., 2011). In our study, the TD temperature of 250°C is lower than the maximum temperature used by the PMP (300-400°C) and does not follow the exact operation specifications of the PMP. However, Amanatidis et al. (2018) summarised that TD is a suitable alternative approach for the removal of volatile particles. Particles larger than 23 nm downstream of the TD were measured by the EEPs and we integrated the size bins from 23.5 nm to 560 nm to represent the SPN. Figure 3b compares the EF_{PM} and EF_{SPN} of Euro VI HDTs. Generally, after-treatment control systems could not reduce SPN emissions as effectively as PM emissions, indicating that more control of SPN emission of Euro VI HDTs may be necessary.

Shown in Table 2 are the average EFs of gaseous pollutants (NO_x , CO, HC) in this study compared with other studies. EF_{NO_x} generally decreased from the Euro III (43.3 g (kg fuel)⁻¹) to Euro VI (3.1 g (kg fuel)⁻¹) class, and are in good agreement with reported values for HDTs in the literature. EF_{NO_x} of Euro III HDTs is moderately higher in this study. Note that the EF_{NO_x} and EF_{PM} of EEV were much higher in Pirjola et al. (2016), in which only a limited number (3-4) vehicles were tested and hard braking was common in approaching a 90° turn before accelerating again. The ratio of EF_{NO_2} to EF_{NO_x} generally agrees with the projection in Kousoulidou et al. (2008), on-road plume chasing measurements in Lau et al. (2015) and remote sensing studies in the UK (Carslaw and Rhys-Tyler, 2013). Carslaw et al. (2019) reported a decreasing trend of EF_{NO_2}/EF_{NO_x} with vehicle mileage for Euro 6 light-duty diesel vehicles, while no significant trend was identified for Euro VI HDTs in this study. There may be other parameters influencing the NO_x emission. For example, Ko et al. (2019) reported that the NO_x emissions from Euro VI diesel vehicles were 29% higher in a traffic jam than in smooth traffic conditions. The temperature of the exhaust and DPF regeneration may also influence the EF_{NO_x} .

Compared with EF_{NO_x} , EF_{CO} decreased less pronounced from Euro III to Euro VI HDTs (57%). Compared with newer Euro class HDTs, a larger fraction of HDTs in older Euro classes have an EF_{CO} exceeding the Euro standards, which indicates that engine deterioration may have a serious effect on the CO emissions (Fig. S8c). Hallquist et al. (2013) reported a positive relationship between EF_{CO} and EF_{PM} , i.e. high CO indicates incomplete combustion which favors soot formation. DPFs may also reduce CO in addition to PM (Hallquist et al., 2013), which is in agreement with the lowest CO emission of 15.5 g (kg fuel)⁻¹ observed for DPF equipped Euro VI HDTs in this study. ~~HC emission was relatively low for all HDT types, but no~~

obvious decreasing trend was evident for EF_{HC} from Euro III to Euro VI HDTs (Fig. S8d and Table 2). HC emission was relatively low for all HDT types, and no obvious decreasing trend was evident for EF_{HC} from Euro III to Euro VI HDTs (Jonckheere-Terpstra test, $p=0.895$) (Fig. S8d and Table 2). This does not reflect the more stringent Euro standard limit regarding HC where the Euro VI limit is more than a factor of three lower than the preceding Euro V/IV standards.

The 46 Swedish HDTs without available Euro type information emitted similar levels of particle and gaseous pollutants to Euro VI HDTs and were thus likely equipped with newer Euro engines.

~~Compared with non-Swedish HDTs, Swedish HDTs generally have lower EFs in terms of all the pollutants (Fig. 2 and Tables 1 and 2), which may be attributed to the more stringent domestic goals regarding pollution, clean air, greenhouse gas emissions, energy efficiency, and innovative sustainable solutions (Government Offices of Sweden, 2017). One may note that the non-Swedish HDTs was not identified according to Euro class and could contain a larger share of non-Euro VI trucks.~~

~~Compared with the fleet of non-Swedish HDTs, the Swedish HDT fleet generally have a lower median and average EF_{NOx} but there are no significant differences in the EF of other pollutants (Fig. 2 and Tables 1 and 2). The differences in EF_{NOx} are significant at the statistical 95% CI using the Kolmogorov-Smirnov test, used in favour to typical student t-test to account for non-normality of the EF distributions. As information of Euro class, engine types and treatment technologies of non-Swedish HDTs is not available, we cannot further explore why there is a difference between the two fleets.~~

~~In addition to engine Euro type, pollutant emission trends were also investigated with respect to five different vehicle manufacturers (M1, M2, M3, M4, and M5). EF_{PM} , EF_{PN} , EF_{BC} and EF_{NOx} of HDTs under the same Euro class but from different manufacturers are compared in Fig. S9. Since EF data was not normally distributed, statistical significance is assessed with a Kruskal-Wallis test. It is a non-parametric analogue of the one-way ANOVA test. The p-values are calculated at the statistical 95% confidence level. No significant group difference ($p>0.05$) was observed in EF_{PM} , EF_{PN} , EF_{BC} , and EF_{NOx} for Euro V HDTs, i.e., HDTs from five different manufacturers show comparable emission characteristics. EF_{PM} , EF_{PN} , and EF_{NOx} of Euro VI HDTs show no dependency on manufacturers, but a significant difference was observed between M2 and M5 in EF_{BC} of Euro VI HDTs ($p=0.016$). (No analysis on Euro III, Euro IV, and EEV HDTs was conducted due to the limited vehicle number from each manufacturer).~~

3.4 Size-resolved EF_{PN} of volatile and non-volatile particles

Figure 4a-e show the average size-resolved number emission factors (solid lines) simultaneously measured via the bypass and TD lines for different Euro class HDTs. The EF_{PN} of the volatile components is calculated as the difference of EF_{PN} measured after the bypass line and the non-volatile component EF_{PN} measured after the TD line. To differentiate between nucleation and accumulation mode particles, a cut point particle diameter of 30 nm was used as defined by Kittelson et al. (2002). In general, all Euro III, Euro IV, Euro V and EEV HDTs showed a bimodal particle number size distribution, with one mode peaking at ~6-10 nm (nucleation mode) and another at ~50-80 nm (accumulation/soot mode) (Maricq, 2007). For Euro VI HDTs the particle number size distributions were dominated by the nucleation mode. The EF_{PN} of the accumulation mode particles shows a decreasing trend from Euro III to EEV HDTs. The accumulation mode of the Euro VI HDTs was insignificant. For heavy-

duty diesel engines without a particulate filter, nucleation mode particles are mainly formed from organics. For vehicles with DPF both organics and the fuel sulphur content might influence the formation of nucleation mode particles (Vaaraslahti et al., 2004). Thiruvengadam et al. (2012) found a direct relationship between exhaust nanoparticles in the nucleation mode and the exhaust temperature of the DPF-SCR equipped diesel engine. These factors lead to high variability in the nucleation mode fraction of EF_{PN} . Figure 4f shows that HDVs with DPF (dashed lines) exhibited lower emissions of accumulation mode particles, with no significant reduction in nucleation mode particles when compared to HDVs without DPF (solid lines). In general, the absence of significant accumulation mode particles from Euro VI HDTs was consistent with observations made from DPF equipped HDVs. High emissions of accumulation mode particles from Euro III HDTs were consistent with measurements from HDVs without DPF in previous studies (Liu et al., 2019; Hallquist et al., 2009; Preble et al., 2015).

Most particles in the nucleation mode evaporate after passing through the TD. Sakurai et al. (2003b) reported that volatile compounds in diesel particles are mainly comprised of unburned lubrication oil. The non-volatile components in the nucleation mode may consist of metallic ash from lubrication oil or fuel additives (Sakurai et al., 2003a) or some organic compounds of extremely low volatility (Gkatzelis et al., 2016). In the accumulation mode, the particle mode diameter shifted towards lower sizes after passing the TD. In Fig. 4, we also present the median size distribution (dashed lines). There is a small difference between mean and median size distributions in the accumulation mode while a bigger difference occurs in the nucleation mode. The latter mode is more dynamic and there are larger possibilities for extreme values skewing the averages.

To be consistent with previous studies which overwhelmingly report average size distributions, we choose to utilize the average size distributions for the discussions below. The volatilities of particle emissions in the accumulation and nucleation mode have been evaluated by calculating the average EF_{PN} and EF_{PM} fraction remaining (after heating) of particles emitted from Euro III-VI HDTs (Fig. S10). In general, the EF_{PN} fraction remaining in the nucleation mode was lower than that in the accumulation mode across all HDTs in all Euro classes. In terms of particle mass, the nucleation mode and accumulation mode showed similar EF_{PM} fractions remaining from Euro III to EEV HDTs, while Euro VI HDTs had a much lower EF_{PM} fraction remaining in the nucleation mode than in the accumulation mode. Compared with other Euro class HDTs, Euro VI HDTs had the lowest EF_{PN} and EF_{PM} fraction remaining in both nucleation and accumulation mode. Around 94% of the particles by number and 55% of the particles by mass (or volume) in total were evaporated. Alföldy et al. (2009) reported that if the same amount of volatile mass in the nucleation mode and accumulation mode were inhaled, 48% and 29% of the mass would deposit in the lung respectively, implying that volatile mass in the nucleation mode would exert a 1.5 times stronger effect.

3.5 Emissions from high emitters

Figure 5 shows the cumulative emission distributions for PM, PN, NO_x , and NO_2 emissions, with HDTs ranked in order from dirtiest to cleanest. The plots show a significant skewedness towards a small fraction of HDTs with a high fraction of total emissions (deviation from 1:1 line) for each pollutant, indicating the importance of “high emitters”. The disproportionate skewed distribution of pollutants is a common feature of on-road emission measurements (Preble et al., 2018; Preble et al., 2015; Dallmann et al., 2012). The highest-emitting 10% of HDTs in each pollutant were responsible for 65% of total PM, 70%

of total PN, 44% of total NO_x emissions and 69% of total NO₂, respectively. The distribution of NO_x has the least skewedness compared with the other pollutants. If the 10% highest emitters for each pollutant were removed, the corresponding average EF for PM, PN, NO_x, and NO₂ would decrease by 62%, 67%, 38%, and 66% respectively. However, the high emitters for each pollutant are different. For example, Euro III HDTs account for 70% and 67% of the top 3% emitters for PM and BC emissions, while Euro VI HDTs account for 80% and 56% of the top 3% emitters for PN and NO₂ emissions. Here, top 3% emitters were chosen as the reference because Euro III HDTs only accounted for 3% of the total number of HDTs. Lau et al. (Lau et al., 2015) similarly reported that not all high-emitters were members of the lower Euro classes and that high-emitters for a particular pollutant may not simultaneously be high-emitters for other pollutants.

3.6 Fleet characteristics

Figure 6a-d show the changes in average EFs of PM, PN, BC, and NO_x with respect to the registration year of the HDTs. Triennial average EFs were calculated, with truck registration years divided into 5 bins (2002-2005, 2006-2008, 2009-2011, 2012-2014 and 2015-2017). The black arrows in Fig. 6d show the years that the particular type of HDTs examined in this study was first registered. Coupled with the possible phase-out of older fleets, the HDTs with more advanced engines gradually accounted for a higher proportion of the total fleet. There is a significant improvement during the last years and the transition to widespread adoption of Euro VI will take real-world on-road emissions into a new era of much lower contributions to air pollution.

To estimate for each Euro class the typical contribution of air pollution emissions we utilised the number of kilometres driven by HDTs on Swedish roads. During 2018, 4.1×10^9 and 9.2×10^8 kilometres were driven by Swedish and non-Swedish diesel HDTs on Swedish roads, contributing to 82% and 18% to the total distances travelled by diesel HDTs respectively (Fig. 7a). The numbers of kilometres driven by Swedish Euro 0, Euro I, Euro II, Euro III, Euro IV, Euro V and Euro VI diesel HDTs were 2.8×10^7 , 5.0×10^6 , 5.4×10^7 , 2.0×10^8 , 3.1×10^8 , 1.3×10^9 and 2.2×10^9 respectively (HBEFA 3.3, 2019). In Figure 7b, the relative contributions of kilometers driven by Swedish Euro 0 to Euro VI HDTs are shown. Zhang et al. (2014) reported no statistically significant difference in fuel consumption among Euro II to Euro IV buses under a real-world typical bus driving cycle in Beijing. In this study, we assume the fuel consumption per kilometre and fuel density are the same across the different Euro class HDTs and adopting the average fuel-based EFs calculated in this study (Tables 1 and 2), the approximation of contributions of pollutants emitted from Swedish HDTs in each Euro class to the total PM, PN, BC and NO_x emissions are depicted in Fig. 7c-f. Due to a lack of corresponding emission information, pollutant average EFs of Euro 0, Euro I and Euro II HDTs were assumed to be at the same level as those of Euro III HDTs representing lower bound estimates. Euro 0-II HDTs accounted for less than 2.2% of the grand total distance driven but totally contributed to 16%, 13%, 6% and 4% of BC, PM, NO_x, and PN emissions. Euro III HDTs only accounted for 5% (Fig. 7b) of the total fleet but disproportionally contributed to 37%, 30%, 16% and 10% of BC, PM, NO_x, and PN emissions. Euro IV HDTs also exhibited disproportionally high PM and NO_x emissions. A fraction of 32% of HDTs belonged to the Euro V category, they contributed to 53%, 42%, 34%, and 32% of NO_x, PM, BC and PN emissions respectively. Upgrading, replacing or making obsolete Euro 0 to Euro V HDTs would be

necessary for mitigating a large part of the PM, PN, BC and NO_x emissions. Euro VI HDTs accounted for the highest fraction of the total fleet (53%), but only contributed to 2%, 6%, 12% and 47% of PM, BC, NO_x, and PN emissions, indicating successful overall pollution reduction with the introduction of more Euro VI HDVs. Using the median EFs as references, the emission contributions from Euro VI HDTs to the total pollutant emissions would be even lower (Fig. S11). These data provide useful information to predict future pollutant emission trends and to guide policy analysis and implementation. Since the predicted transition in emissions from road transport would be significant, chemical transport model/cost-assessment models need to get fast access to emission factors for new generation HDTs to be able to provide a better estimation of near future air pollution levels.

4 Atmospheric implications and conclusions

The transition in the atmospheric emission of particles and gases from on-road HDTs caused by the modernisation of the fleet is reported in this study. ~~Particle emissions of PM, BC and to a lesser extent PN exhibited substantial reductions from Euro III to Euro VI HDTs. The gaseous emissions of NO_x and CO also showed significant decrease with respect to Euro class, while the HC emission was relatively low for all the HDT Euro class types. Particle emissions of PM, BC and to a lesser extent PN exhibited substantial reductions from Euro III to Euro VI HDTs (Jonckheere-Terpstra test, $p < 0.01$). The gaseous emissions of NO_x and CO also showed a significant decrease with respect to Euro class (Jonckheere-Terpstra test, $p < 0.01$), while the HC emission was relatively low for all the HDT Euro class types.~~ Compared with Euro III HDTs, Euro VI HDTs showed 99%, 98%, 93% and 57% reductions of the average emissions factors of PM, BC, NO_x, and CO respectively. Although a significant reduction in NO_x emissions and a lower median EF_{NO2} were evident, the fraction of NO₂ in the NO_x emissions increased continuously from Euro IV to Euro VI HDTs, and Euro VI HDTs were the dominant class of the top 3% emitters for NO₂. PN showed the largest data scattering for Euro VI HDTs, though after evaporation of the volatile fraction, SPN became less scattered. A plausible reason for this large variability in PN but not PM is the formation of nucleation mode particles containing more volatile compounds, which is more sensitive to individual driving and plume dilution conditions. Reducing particle mass by DPF is clearly important but the consequence in doing so removes particle surface area available for condensation and may therefore favour nucleation mode particle formation if not the precursors of these are also reduced. Furthermore, due to the absence of larger particles, the coagulation rate is decreased and produced nucleation mode particle can retain for a longer time in the atmosphere, which has a direct influence on the evaluation of near-road human exposure.

Driving condition and engine technology affected the size distribution of particle number emissions. The average particle number size distributions of Euro III to EEV HDTs were bimodal with nucleation modes at ~6-10 nm and accumulation modes at ~50-80 nm. Euro VI HDTs displayed nucleation mode dominant size distributions. Measurements of particle volatility revealed that Euro VI HDTs had the highest volatile fraction in both nucleation mode and accumulation mode compared to the other Euro classes. More detailed chemical composition information of this volatile fraction is needed to assess their potential impacts for health and formation of SOA.

We also found that a small number of high emitters contributed to a large fraction of the total emissions. The top 10% emitters in each pollutant category were responsible for 65% of total PM, 70% of total PN, 44% of total NO_x and 69% of total NO₂ emissions, respectively. Euro III HDTs were the dominant top 3% emitters for PM and BC emissions, and Euro VI HDTs were the dominant top 3% emitters for PN and NO₂ emissions.

In general, an overall pollution reduction has been achieved during the last years and the transition to Euro VI adoption will take real-world on-road emissions into a new era of much lower contributions to air pollution. The emissions of PM, BC and NO_x are predicted to further decrease in the future, while PN emissions may be subject to greater fluctuation and therefore be more challenging to control. Upgrading or phasing-out of existing Euro 0 to Euro V vehicles and introducing more Euro VI HDTs would result in large pollution reductions. More intensive attentions need to be focused on SPN controls for Euro VI HDTs. A careful and more detailed examination of the impacts of fleet upgrades in terms of ambient pollutant levels and emission reduction targets for individual pollutants may be needed for further evaluation.

Data availability.

The data used in this publication are available to the community and can be accessed by request to the corresponding author.

Author contributions.

ÅMH designed the project; LZ, ÅMH, CMS, SMG, ÅS, MJ, HS, MH, and IW conducted the measurements; LZ, CMS, and QL analysed data; LZ, ÅMH, MH, CKC and BPL wrote the paper. All co-authors contributed to the discussion of the manuscript.

Competing interests.

The authors declare that they have no conflict of interest.

Acknowledgments.

This work was financed by Formas (214-2013-1430) and was an initiative within the framework programme “Photochemical smog in China” financed by the Swedish Research Council (639-2013-6917). Chak K. Chan would like to acknowledge the support of the Science Technology and Innovation Committee of Shenzhen Municipality (project no. JCYJ20160401095857424).

References

- Alfoldy, B., Giechaskiel, B., Hofmann, W., and Drossinos, Y.: Size-distribution dependent lung deposition of diesel exhaust particles, *J. Aerosol Sci.*, 40, 652-663, 10.1016/j.jaerosci.2009.04.009, 2009.
- Amanatidis, S., Ntziachristos, L., Karjalainen, P., Saukko, E., Simonen, P., Kuittinen, N., Aakko-Saksa, P., Timonen, H., Ronkko, T., and Keskinen, J.: Comparative performance of a thermal denuder and a catalytic stripper in sampling laboratory and marine exhaust aerosols, *Aerosol Sci. Tech.*, 52, 420-432, <https://doi.org/10.1080/02786826.2017.1422236>, 2018.

489 Arnold, F., Pirjola, L., Ronkko, T., Reichl, U., Schlager, H., Lahde, T., Heikkila, J., and Keskinen, J.: First online
 490 measurements of sulfuric acid gas in modern heavy-duty diesel engine exhaust: implications for nanoparticle formation,
 491 *Environ. Sci. Technol.*, 46, 11227-11234, <https://doi.org/10.1021/es302432s>, 2012.

492 Ban-Weiss, G. A., Lunden, M. M., Kirchstetter, T. W., and Harley, R. A.: Measurement of black carbon and particle number
 493 emission factors from individual heavy-duty trucks, *Environ. Sci. Technol.*, 43, 1419-1424, <https://doi.org/10.1021/es8021039>,
 494 2009.

495 Bergmann, M., Kirchner, U., Vogt, R., and Benter, T.: On-road and laboratory investigation of low-level PM emissions of a
 496 modern diesel particulate filter equipped diesel passenger car, *Atmos. Environ.*, 43, 1908-1916,
 497 <https://doi.org/10.1016/j.atmosenv.2008.12.039>, 2009.

498 Bishop, G. A., and Stedman, D. H.: A decade of on-road emissions measurements, *Environ. Sci. Technol.*, 42, 1651-1656,
 499 <https://doi.org/10.1021/es702413b>, 2008.

500 Bishop, G. A., Peddle, A. M., Stedman, D. H., and Zhan, T.: On-road emission measurements of reactive nitrogen compounds
 501 from three California cities, *Environ. Sci. Technol.*, 44, 3616-3620, <https://doi.org/10.1021/es903722p>, 2010.

502 Bishop, G. A., Schuchmann, B. G., and Stedman, D. H.: Heavy-duty truck emissions in the South Coast Air Basin of California,
 503 *Environ. Sci. Technol.*, 47, 9523-9529, <https://doi.org/10.1021/es401487b>, 2013.

504 Bishop, G. A., Hottor-Raguindin, R., Stedman, D. H., McClintock, P., Theobald, E., Johnson, J. D., Lee, D. W., Zietsman, J.,
 505 and Misra, C.: On-road heavy-duty vehicle emissions monitoring system, *Environ. Sci. Technol.*, 49, 1639-1645,
 506 <https://doi.org/10.1021/es505534e>, 2015.

507 Biswas, S., Verma, V., Schauer, J. J., Cassee, F. R., Cho, A. K., and Sioutas, C.: Oxidative potential of semi-volatile and non-
 508 volatile particulate matter (PM) from heavy-duty vehicles retrofitted with emission control technologies, *Environ. Sci.*
 509 *Technol.*, 43, 3905-3912, <https://doi.org/10.1021/es9000592>, 2009.

510 Bocchi, C., Bazzini, C., Fontana, F., Pinto, G., Martino, A., and Cassoni, F.: Characterization of urban aerosol: seasonal
 511 variation of mutagenicity and genotoxicity of PM_{2.5}, PM₁ and semi-volatile organic compounds, *Mutat. Res.*, 809, 16-23,
 512 <https://doi.org/10.1016/j.mrgentox.2016.07.007>, 2016.

513 Burgard, D. A., Bishop, G. A., Stedman, D. H., Gessner, V. H., and Daeschlein, C.: Remote sensing of in-use heavy-duty
 514 diesel trucks, *Environ. Sci. Technol.*, 40, 6938-6942, <https://doi.org/10.1021/es060989a>, 2006.

515 Burgard, D. A., and Provinsal, M. N.: On-road, in-use gaseous emission measurements by remote sensing of school buses
 516 equipped with diesel oxidation catalysts and diesel particulate filters, *J. Air Waste Manag. Assoc.*, 59, 1468-1473,
 517 <https://doi.org/10.3155/1047-3289.59.12.1468>, 2009.

518 Campagnolo, D., Cattaneo, A., Corbella, L., Borghi, F., Del Buono, L., Rovelli, S., Spinazze, A., and Cavallo, D. M.: In-
 519 vehicle airborne fine and ultra-fine particulate matter exposure: The impact of leading vehicle emissions, *Environ. Int.*, 123,
 520 407-416, <https://doi.org/10.1016/j.envint.2018.12.020>, 2019.

521 Carslaw, D. C., Beevers, S. D., Tate, J. E., Westmoreland, E. J., and Williams, M. L.: Recent evidence concerning higher NO_x
 522 emissions from passenger cars and light-duty vehicles, *Atmos. Environ.*, 45, 7053-7063,
 523 <https://doi.org/10.1016/j.atmosenv.2011.09.063>, 2011.

524 Carslaw, D. C., and Rhys-Tyler, G.: New insights from comprehensive on-road measurements of NO_x, NO₂ and NH₃ from
525 vehicle emission remote sensing in London, UK, *Atmos. Environ.*, 81, 339-347,
526 <https://doi.org/10.1016/j.atmosenv.2013.09.026>, 2013.

527 Carslaw, D. C., Farren, N. J., Vaughan, A. R., Drysdale, W. S., Young, S., and Lee, J. D.: The diminishing importance of
528 nitrogen dioxide emissions from road vehicle exhaust, *Atmospheric Environment: X*, 1, 100002,
529 <https://doi.org/10.1016/j.aeaoa.2018.100002>, 2019.

530 Chen, L., Wang, Z., Liu, S., and Qu, L.: Using a chassis dynamometer to determine the influencing factors for the emissions
531 of Euro VI vehicles, *Transport. Res. D- Tr. E.*, 65, 564-573, <https://doi.org/10.1016/j.trd.2018.09.022>, 2018.

532 Cheung, H. H. Y., Tan, H. B., Xu, H. B., Li, F., Wu, C., Yu, J. Z., and Chan, C. K.: Measurements of non-volatile aerosols
533 with a VTDMA and their correlations with carbonaceous aerosols in Guangzhou, China, *Atmos.*
534 *Chem. Phys.*, 16, 8431-8446, <https://doi.org/10.5194/acp-16-8431-2016>, 2016.

535 Clark, N. N., Gautam, M., Rapp, B. L., Lyons, D. W., Graboski, M. S., McCormick, R. L., Alleman, T. L., and Norton, P.:
536 Diesel and CNG transit bus emissions characterization by two chassis dynamometer laboratories: Results and issues, *SAE*
537 *Technical Paper*, 0148-7191, 1999.

538 Cui, M., Chen, Y. J., Feng, Y. L., Li, C., Zheng, J. Y., Tian, C. G., Yan, C. Q., and Zheng, M.: Measurement of PM and its
539 chemical composition in real-world emissions from non-road and on-road diesel vehicles, *Atmos.*
540 *Chem. Phys.*, 17, 6779-6795, <https://doi.org/10.5194/acp-17-6779-2017>, 2017.

541 Dallmann, T. R., DeMartini, S. J., Kirchstetter, T. W., Herndon, S. C., Onasch, T. B., Wood, E. C., and Harley, R. A.: On-road
542 measurement of gas and particle-phase pollutant emission factors for individual heavy-duty diesel trucks, *Environ. Sci.*
543 *Technol.*, 46, 8511-8518, <https://doi.org/10.1021/es301936c>, 2012.

544 Donahue, N. M., Robinson, A. L., Stanier, C. O., and Pandis, S. N.: Coupled partitioning, dilution, and chemical aging of
545 semivolatile organics, *Environ. Sci. Technol.*, 40, 2635-2643, <https://doi.org/10.1021/es052297c>, 2006.

546 Dreher, D. B., and Harley, R. A.: A fuel-based inventory for heavy-duty diesel truck emissions, *J. Air Waste Manage.*, 48,
547 352-358, <https://doi.org/10.1080/10473289.1998.10463686>, 1998.

548 Du, Y., Xu, X., Chu, M., Guo, Y., and Wang, J.: Air particulate matter and cardiovascular disease: the epidemiological,
549 biomedical and clinical evidence, *J. Thorac. Dis.*, 8, E8-E19, <http://dx.doi.org/10.3978/j.issn.2072-1439.2015.11.37> 2016.

550 Edwards, R., Larivé, J., Rickeard, D., and Weindorf, W.: Well-to-Wheels analysis of future automotive fuels and powertrains
551 in the European context: Well-to-Tank Appendix 2-Version 4a, Joint Research Centre of the European Commission, EUCAR,
552 and CONCAWE, 1-133, <http://10.2790/95629>, 2014.

553 EEA: Air Quality in Europe - 2018 Report, 2018.

554 Franco, V., Kousoulidou, M., Muntean, M., Ntziachristos, L., Hausberger, S., and Dilara, P.: Road vehicle emission factors
555 development: A review, *Atmos. Environ.*, 70, 84-97, <https://doi.org/10.1016/j.atmosenv.2013.01.006>, 2013.

556 Gentner, D. R., Jathar, S. H., Gordon, T. D., Bahreini, R., Day, D. A., El Haddad, I., Hayes, P. L., Pieber, S. M., Platt, S. M.,
557 de Gouw, J., Goldstein, A. H., Harley, R. A., Jimenez, J. L., Prevot, A. S., and Robinson, A. L.: Review of Urban Secondary
558 Organic Aerosol Formation from Gasoline and Diesel Motor Vehicle Emissions, *Environ. Sci. Technol.*, 51, 1074-1093,
559 <https://doi.org/10.1021/acs.est.6b04509>, 2017.

560 Gertler, A. W.: Diesel vs. gasoline emissions: Does PM from diesel or gasoline vehicles dominate in the US?, *Atmos. Environ.*,
561 39, 2349-2355, <https://doi.org/10.1016/j.atmosenv.2004.05.065>, 2005.

562 Giechaskiel, B., Alfoldy, B., and Drossinos, Y.: A metric for health effects studies of diesel exhaust particles, *J. Aerosol Sci.*,
563 40, 639-651, <https://doi.org/10.1016/j.jaerosci.2009.04.008>, 2009.

564 Giechaskiel, B., Mamakos, A., Andersson, J., Dilara, P., Martini, G., Schindler, W., and Bergmann, A.: Measurement of
565 Automotive Nonvolatile Particle Number Emissions within the European Legislative Framework: A Review, *Aerosol Sci.*
566 *Tech.*, 46, 719-749, <https://doi.org/10.1080/02786826.2012.661103>, 2012.

567 Giechaskiel, B., Schwelberger, M., Delacroix, C., Marchetti, M., Feijen, M., Prieger, K., Andersson, S., and Karlsson, H. L.:
568 Experimental assessment of solid particle number Portable Emissions Measurement Systems (PEMS) for heavy-duty vehicles
569 applications, *J. Aerosol Sci.*, 123, 161-170, <https://doi.org/10.1016/j.jaerosci.2018.06.014>, 2018.

570 Gkatzelis, G. I., Papanastasiou, D. K., Florou, K., Kaltsonoudis, C., Louvaris, E., and Pandis, S. N.: Measurement of
571 nonvolatile particle number size distribution, *Atmos. Meas. Tech.*, 9, 103-114, <https://doi.org/10.5194/amt-9-103-2016>, 2016.

572 ~~The climate policy framework: <http://www.government.se/articles/2017/06/the-climate-policy-framework/>, 2017.~~

573 Grigoratos, T., Fontaras, G., Giechaskiel, B., and Zacharof, N.: Real-world emissions performance of heavy-duty Euro VI
574 diesel vehicles, *Atmos. Environ.*, 201, 348-359, <https://doi.org/10.1016/j.atmosenv.2018.12.042>, 2019.

575 Guo, J. D., Ge, Y. S., Hao, L. J., Tan, J. W., Li, J. Q., and Feng, X. Y.: On-road measurement of regulated pollutants from
576 diesel and CNG buses with urea selective catalytic reduction systems, *Atmos. Environ.*, 99, 1-9,
577 <https://doi.org/10.1016/j.atmosenv.2014.07.032>, 2014.

578 Hak, C. S., Hallquist, M., Ljungstrom, E., Svane, M., and Pettersson, J. B. C.: A new approach to in-situ determination of
579 roadside particle emission factors of individual vehicles under conventional driving conditions, *Atmos. Environ.*, 43, 2481-
580 2488, <https://doi.org/10.1016/j.atmosenv.2009.01.041>, 2009.

581 Hallquist, A. M., Jerksjo, M., Fallgren, H., Westerlund, J., and Sjodin, A.: Particle and gaseous emissions from individual
582 diesel and CNG buses, *Atmos. Chem. Phys.*, 13, 5337-5350, <https://doi.org/10.5194/acp-13-5337-2013>, 2013.

583 Hallquist, M., Wenger, J. C., Baltensperger, U., Rudich, Y., Simpson, D., Claeys, M., Dommen, J., Donahue, N. M., George,
584 C., Goldstein, A. H., Hamilton, J. F., Herrmann, H., Hoffmann, T., Iinuma, Y., Jang, M., Jenkin, M. E., Jimenez, J. L., Kiendler-
585 Scharr, A., Maenhaut, W., McFiggans, G., Mentel, T. F., Monod, A., Prevot, A. S. H., Seinfeld, J. H., Surratt, J. D., Szmigielski,
586 R., and Wildt, J.: The formation, properties and impact of secondary organic aerosol: current and emerging issues, *Atmos.*
587 *Chem. Phys.*, 9, 5155-5236, <https://doi.org/10.5194/acp-9-5155-2009>, 2009.

588 Haugen, M. J., Bishop, G. A., Thiruvengadam, A., and Carder, D. K.: Evaluation of Heavy-and Medium-Duty On-Road
589 Vehicle Emissions in California's South Coast Air Basin, *Environ. Sci. Technol.*, 52, 13298-13305,
590 <https://doi.org/10.1021/acs.est.8b03994>, 2018.

591 He, C., Li, J., Ma, Z., Tan, J., and Zhao, L.: High NO₂/NO_x emissions downstream of the catalytic diesel particulate filter: An
592 influencing factor study, *J. Environ. Sci. (China)*, 35, 55-61, <https://doi.org/10.1016/j.jes.2015.02.009>, 2015.

593 He, L., Hu, J., Zhang, S., Wu, Y., Guo, X., Guo, X., Song, J., Zu, L., Zheng, X., and Bao, X.: Investigating real-world emissions
594 of China's heavy-duty diesel trucks: Can SCR effectively mitigate NO_x emissions for highway trucks, *Aerosol Air. Qual. Res.*,
595 17, 2585-2594, <https://DOI: 10.4209/aaqr.2016.12.0531>, 2017.

596 Heeb, N. V., Schmid, P., Kohler, M., Gujer, E., Zennegg, M., Wenger, D., Wichser, A., Ulrich, A., Gfeller, U., Honegger, P.,
597 Zeyer, K., Emmenegger, L., Petermann, J. L., Czerwinski, J., Mosimann, T., Kasper, M., and Mayer, A.: Impact of low- and
598 high-oxidation diesel particulate filters on genotoxic exhaust constituents, *Environ. Sci. Technol.*, 44, 1078-1084,
599 <https://doi.org/10.1021/es9019222>, 2010.

600 Herner, J. D., Hu, S., Robertson, W. H., Huai, T., Collins, J. F., Dwyer, H., and Ayala, A.: Effect of advanced aftertreatment
601 for PM and NO_x control on heavy-duty diesel truck emissions, *Environ. Sci. Technol.*, 43, 5928-5933,
602 <https://doi.org/10.1021/es9008294>, 2009.

603 Herner, J. D., Hu, S., Robertson, W. H., Huai, T., Chang, M.-C. O., Rieger, P., and Ayala, A.: Effect of advanced aftertreatment
604 for PM and NO_x reduction on heavy-duty diesel engine ultrafine particle emissions, *Environ. Sci. Technol.*, 45, 2413-2419,
605 <https://doi.org/10.1021/es102792y>, 2011.

606 Heywood, J. B.: *Internal combustion engine fundamentals*, 1988.

607 Huffman, J. A., Ziemann, P. J., Jayne, J. T., Worsnop, D. R., and Jimenez, J. L.: Development and characterization of a fast-
608 stepping/scanning thermodenuder for chemically-resolved aerosol volatility measurements, *Aerosol Sci. Tech.*, 42, 395-407,
609 <https://doi.org/10.1080/02786820802104981>, 2008.

610 Janhall, S., and Hallquist, M.: A novel method for determination of size-resolved, submicrometer particle traffic emission
611 factors, *Environ. Sci. Technol.*, 39, 7609-7615, <https://doi.org/10.1021/es048208y>, 2005.

612 Jarvinen, A., Timonen, H., Karjalainen, P., Bloss, M., Simonen, P., Saarikoski, S., Kuuluvainen, H., Kalliokoski, J., Dal Maso,
613 M., Niemi, J. V., Keskinen, J., and Ronkko, T.: Particle emissions of Euro VI, EEV and retrofitted EEV city buses in real
614 traffic, *Environ. Pollut.*, 250, 708-716, <https://doi.org/10.1016/j.envpol.2019.04.033>, 2019.

615 Jiang, Y., Yang, J., Cocker, D., 3rd, Karavalakis, G., Johnson, K. C., and Durbin, T. D.: Characterizing emission rates of
616 regulated pollutants from model year 2012+ heavy-duty diesel vehicles equipped with DPF and SCR systems, *Sci. Total
617 Environ.*, 619-620, 765-771, <https://doi.org/10.1016/j.scitotenv.2017.11.120>, 2018.

618 Kittelson, D., Watts, W., and Johnson, J.: *Diesel Aerosol Sampling Methodology—CRC E-43*, Final report, Coordinating
619 Research Council, 2002.

620 Ko, J., Myung, C. L., and Park, S.: Impacts of ambient temperature, DPF regeneration, and traffic congestion on NO_x emissions
621 from a Euro 6-compliant diesel vehicle equipped with an LNT under real-world driving conditions, *Atmos. Environ.*, 200, 1-
622 14, <https://doi.org/10.1016/j.atmosenv.2018.11.029>, 2019.

623 Kousoulidou, M., Ntziachristos, L., Mellios, G., and Samaras, Z.: Road-transport emission projections to 2020 in European
624 urban environments, *Atmos. Environ.*, 42, 7465-7475, <https://doi.org/10.1016/j.atmosenv.2008.06.002>, 2008.

625 Kozawa, K. H., Park, S. S., Mara, S. L., and Herner, J. D.: Verifying emission reductions from heavy-duty diesel trucks
626 operating on Southern California freeways, *Environ. Sci. Technol.*, 48, 1475-1483, <https://doi.org/10.1021/es4044177>, 2014.

627 Lau, C. F., Rakowska, A., Townsend, T., Brimblecombe, P., Chan, T. L., Yam, Y. S., Mocnik, G., and Ning, Z.: Evaluation
628 of diesel fleet emissions and control policies from plume chasing measurements of on-road vehicles, *Atmos. Environ.*, 122,
629 171-182, <https://doi.org/10.1016/j.atmosenv.2015.09.048>, 2015.

630 Le Breton, M., Psichoudaki, M., Hallquist, M., Watne, Å., Lutz, A., and Hallquist, Å.: Application of a FIGAERO ToF CIMS
631 for on-line characterization of real-world fresh and aged particle emissions from buses, *Aerosol Sci. Tech.*, 1-16,
632 <https://doi.org/10.1080/02786826.2019.1566592>, 2019.

633 Lee, B. H., Lopez-Hilfiker, F. D., Mohr, C., Kurten, T., Worsnop, D. R., and Thornton, J. A.: An iodide-adduct high-resolution
634 time-of-flight chemical-ionization mass spectrometer: application to atmospheric inorganic and organic compounds, *Environ.*
635 *Sci. Technol.*, 48, 6309-6317, <https://doi.org/10.1021/es500362a>, 2014.

636 Li, X., Dallmann, T. R., May, A. A., Stanier, C. O., Grieshop, A. P., Lipsky, E. M., Robinson, A. L., and Presto, A. A.: Size
637 distribution of vehicle emitted primary particles measured in a traffic tunnel, *Atmos. Environ.*, 191, 9-18,
638 <https://doi.org/10.1016/j.atmosenv.2018.07.052>, 2018.

639 Liu, Q., Hallquist, Å. M., Fallgren, H., Jerksjö, M., Jutterström, S., Salberg, H., Hallquist, M., Le Breton, M., Pei, X., and
640 Pathak, R. K.: Roadside assessment of a modern city bus fleet: Gaseous and particle emissions, *Atmospheric Environment: X*,
641 100044, <https://doi.org/10.1016/j.aeaoa.2019.100044>, 2019.

642 Liu, Z. G., Vasys, V. N., Dettmann, M. E., Schauer, J. J., Kittelson, D. B., and Swanson, J.: Comparison of Strategies for the
643 Measurement of Mass Emissions from Diesel Engines Emitting Ultra-Low Levels of Particulate Matter, *Aerosol Sci. Tech.*,
644 43, 1142-1152, <https://doi.org/10.1080/02786820903219035>, 2009.

645 Lv, Y., Li, X., Xu, T. T., Cheng, T. T., Yang, X., Chen, J. M., Iinuma, Y., and Herrmann, H.: Size distributions of polycyclic
646 aromatic hydrocarbons in urban atmosphere: sorption mechanism and source contributions to respiratory deposition, *Atmos.*
647 *Chem. Phys.*, 16, 2971-2983, <https://doi.org/10.5194/acp-16-2971-2016>, 2016.

648 Mahmoudzadeh Andwari, A., Pesiridis, A., Esfahanian, V., Salavati-Zadeh, A., Karvountzis-Kontakiotis, A., and
649 Muralidharan, V.: A comparative study of the effect of turbo compounding and ORC waste heat recovery systems on the
650 performance of a turbocharged heavy-duty diesel engine, *Energies*, 10, 1087, <https://doi.org/10.3390/en10081087>, 2017.

651 Manigrasso, M., Vernale, C., and Avino, P.: Traffic aerosol lobar doses deposited in the human respiratory system, *Environ.*
652 *Sci. Pollut. Res. Int.*, 24, 13866-13873, <https://doi.org/10.1007/s11356-015-5666-1>, 2017.

653 Maricq, M. M., and Ning, X.: The effective density and fractal dimension of soot particles from premixed flames and motor
654 vehicle exhaust, *J. Aerosol Sci.*, 35, 1251-1274, <https://doi.org/10.1016/j.jaerosci.2004.05.002>, 2004.

655 Maricq, M. M.: Chemical characterization of particulate emissions from diesel engines: A review, *J. Aerosol Sci.*, 38, 1079-
656 1118, <https://doi.org/10.1016/j.jaerosci.2007.08.001>, 2007.

657 Martinet, S., Liu, Y., Louis, C., Tassel, P., Perret, P., Chaumond, A., and Andre, M.: Euro 6 Unregulated Pollutant
658 Characterization and Statistical Analysis of After-Treatment Device and Driving-Condition Impact on Recent Passenger-Car
659 Emissions, *Environ. Sci. Technol.*, 51, 5847-5855, <https://doi.org/10.1021/acs.est.7b00481>, 2017.

660 Martini, G., Giechaskiel, B., and Dilara, P.: Future European emission standards for vehicles: the importance of the UN-ECE
661 Particle Measurement Programme, *Biomarkers*, 14 Suppl 1, 29-33, <https://doi.org/10.1080/13547500902965393>, 2009.

662 May, A. A., Nguyen, N. T., Presto, A. A., Gordon, T. D., Lipsky, E. M., Karve, M., Gutierrez, A., Robertson, W. H., Zhang,
663 M., Brandow, C., Chang, O., Chen, S. Y., Cicero-Fernandez, P., Dinkins, L., Fuentes, M., Huang, S. M., Ling, R., Long, J.,
664 Maddox, C., Massetti, J., McCauley, E., Miguel, A., Na, K., Ong, R., Pang, Y. B., Rieger, P., Sax, T., Truong, T., Vo, T.,
665 Chattopadhyay, S., Maldonado, H., Maricq, M. M., and Robinson, A. L.: Gas- and particle-phase primary emissions from in-
666 use, on-road gasoline and diesel vehicles, *Atmos. Environ.*, 88, 247-260, <https://doi.org/10.1016/j.atmosenv.2014.01.046>,
667 2014.

668 Mendoza-Villafuerte, P., Suarez-Bertoa, R., Giechaskiel, B., Riccobono, F., Bulgheroni, C., Astorga, C., and Perujo, A.: NO_x,
669 NH₃, N₂O and PN real driving emissions from a Euro VI heavy-duty vehicle. Impact of regulatory on-road test conditions on
670 emissions, *Sci. Total Environ.*, 609, 546-555, <https://doi.org/10.1016/j.scitotenv.2017.07.168>, 2017.

671 Moody, A., and Tate, J.: In Service CO₂ and NO_x Emissions of Euro 6/VI Cars, Light-and Heavy-duty goods Vehicles in Real
672 London driving: Taking the Road into the Laboratory, *Journal of Earth Sciences and Geotechnical Engineering*, 7, 51-62,
673 <https://orcid.org/0000-0003-1646-6852>, 2017.

674 Nelson, P. F., Tibbett, A. R., and Day, S. J.: Effects of vehicle type and fuel quality on real-world toxic emissions from diesel
675 vehicles, *Atmos. Environ.*, 42, 5291-5303, <https://doi.org/10.1016/j.atmosenv.2008.02.049>, 2008.

676 Pirjola, L., Ditttrich, A., Niemi, J. V., Saarikoski, S., Timonen, H., Kuuluvainen, H., Jarvinen, A., Kousa, A., Ronkko, T., and
677 Hillamo, R.: Physical and Chemical Characterization of Real-World Particle Number and Mass Emissions from City Buses in
678 Finland, *Environ. Sci. Technol.*, 50, 294-304, <https://doi.org/10.1021/acs.est.5b04105>, 2016.

679 Pirjola, L., Niemi, J. V., Saarikoski, S., Aurela, M., Enroth, J., Carbone, S., Saarnio, K., Kuuluvainen, H., Kousa, A., Ronkko,
680 T., and Hillamo, R.: Physical and chemical characterization of urban winter-time aerosols by mobile measurements in Helsinki,
681 Finland, *Atmos. Environ.*, 158, 60-75, <https://doi.org/10.1016/j.atmosenv.2017.03.028>, 2017.

682 Preble, C., Cados, T., Harley, R., and Kirchstetter, T.: Impacts of Aging Emission Control Systems on In-Use Heavy-Duty
683 Diesel Truck Emission Rates, AGU Fall Meeting Abstracts, 2017,

684 Preble, C. V., Dallmann, T. R., Kreisberg, N. M., Hering, S. V., Harley, R. A., and Kirchstetter, T. W.: Effects of Particle
685 Filters and Selective Catalytic Reduction on Heavy-Duty Diesel Drayage Truck Emissions at the Port of Oakland, *Environ.*
686 *Sci. Technol.*, 49, 8864-8871, <https://doi.org/10.1021/acs.est.5b01117>, 2015.

687 Preble, C. V., Cados, T. E., Harley, R. A., and Kirchstetter, T. W.: In-Use Performance and Durability of Particle Filters on
688 Heavy-Duty Diesel Trucks, *Environ. Sci. Technol.*, 52, 11913-11921, <https://doi.org/10.1021/acs.est.8b02977>, 2018.

689 Quiros, D. C., Hu, S. H., Hu, S. S., Lee, E. S., Sardar, S., Wang, X. L., Olfert, J. S., Jung, H. J. S., Zhu, Y. F., and Huai, T.:
690 Particle effective density and mass during steady-state operation of GDI, PFI, and diesel passenger cars, *J. Aerosol Sci.*, 83,
691 39-54, <https://doi.org/10.1016/j.jaerosci.2014.12.004>, 2015.

692 Quiros, D. C., Thiruvengadam, A., Pradhan, S., Besch, M., Thiruvengadam, P., Demirgok, B., Carder, D., Oshinuga, A., Huai,
693 T., and Hu, S.: Real-world emissions from modern heavy-duty diesel, natural gas, and hybrid diesel trucks operating along
694 major California freight corridors, *Emission Control Science and Technology*, 2, 156-172, [https://doi.org/10.1007/s40825-](https://doi.org/10.1007/s40825-016-0044-0)
695 016-0044-0, 2016.

696 Quiros, D. C., Smith, J. D., Ham, W. A., Robertson, W. H., Huai, T., Ayala, A., and Hu, S.: Deriving fuel-based emission
697 factor thresholds to interpret heavy-duty vehicle roadside plume measurements, *J. Air Waste Manag. Assoc.*, 68, 969-987,
698 <https://doi.org/10.1080/10962247.2018.1460637>, 2018.

699 Rexeis, M., Röck, M., and Hausberger, S.: Comparison of Fuel Consumption and Emissions for Representative Heavy-Duty
700 Vehicles in Europe, 2018.

701 Ristimäki, J., Vaaraslahti, K., Lappi, M., and Keskinen, J.: Hydrocarbon condensation in heavy-duty diesel exhaust, *Environ.*
702 *Sci. Technol.*, 41, 6397-6402, <https://doi.org/10.1021/es0624319>, 2007.

703 Robinson, A. L., Donahue, N. M., Shrivastava, M. K., Weitkamp, E. A., Sage, A. M., Grieshop, A. P., Lane, T. E., Pierce, J.
704 R., and Pandis, S. N.: Rethinking organic aerosols: semivolatile emissions and photochemical aging, *Science*, 315, 1259-1262,
705 <https://doi.org/10.1126/science.1133061>, 2007.

706 Rymaniak, L., Ziolkowski, A., and Gallas, D.: Particle number and particulate mass emissions of heavy-duty vehicles in real
707 operating conditions, *MATEC Web of Conferences*, 2017, 00025,

708 Sakurai, H., Park, K., McMurry, P. H., Zarling, D. D., Kittelson, D. B., and Ziemann, P. J.: Size-dependent mixing
709 characteristics of volatile and nonvolatile components in diesel exhaust aerosols, *Environ. Sci. Technol.*, 37, 5487-5495,
710 <https://doi.org/10.1021/es034362t>, 2003a.

711 Sakurai, H., Tobias, H. J., Park, K., Zarling, D., Docherty, K. S., Kittelson, D. B., McMurry, P. H., and Ziemann, P. J.: On-
712 line measurements of diesel nanoparticle composition and volatility, *Atmos. Environ.*, 37, 1199-1210,
713 [https://doi.org/10.1016/S1352-2310\(02\)01017-8](https://doi.org/10.1016/S1352-2310(02)01017-8), 2003b.

714 Smit, R., Keramydas, C., Ntziachristos, L., Lo, T. S., Ng, K. L., Wong, H. L. A., and Wong, C.: Evaluation of real-world
715 gaseous emissions performance of SCR and DPF bus retrofits, *Environ. Sci. Technol.*, <https://doi.org/10.1021/acs.est.8b07223>,
716 2019.

717 Tan, Y., Henderick, P., Yoon, S., Herner, J., Montes, T., Boriboonsomsin, K., Johnson, K., Scora, G., Sandez, D., and Durbin,
718 T. D.: On-Board Sensor-Based NO_x Emissions from Heavy-Duty Diesel Vehicles, *Environ. Sci. Technol.*, 53, 5504-5511,
719 <https://doi.org/10.1021/acs.est.8b07048>, 2019.

720 Thiruvengadam, A., Besch, M. C., Carder, D. K., Oshinuga, A., and Gautam, M.: Influence of real-world engine load
721 conditions on nanoparticle emissions from a DPF and SCR equipped heavy-duty diesel engine, *Environ. Sci. Technol.*, 46,
722 1907-1913, <https://doi.org/10.1021/es203079n>, 2012.

723 Thiruvengadam, A., Besch, M. C., Thiruvengadam, P., Pradhan, S., Carder, D., Kappanna, H., Gautam, M., Oshinuga, A.,
724 Hogo, H., and Miyasato, M.: Emission rates of regulated pollutants from current technology heavy-duty diesel and natural gas
725 goods movement vehicles, *Environ. Sci. Technol.*, 49, 5236-5244, <https://doi.org/10.1021/acs.est.5b00943>, 2015.

726 Vaaraslahti, K., Virtanen, A., Ristimäki, J., and Keskinen, J.: Nucleation mode formation in heavy-duty diesel exhaust with
727 and without a particulate filter, *Environ. Sci. Technol.*, 38, 4884-4890, <https://doi.org/10.1021/es0353255>, 2004.

728 Van Setten, B. A., Makkee, M., and Moulijn, J. A.: Science and technology of catalytic diesel particulate filters, *Catalysis*
729 *Reviews*, 43, 489-564, <https://doi.org/10.1081/CR-120001810>, 2001.

730 Vojtisek-Lom, M., Pechout, M., Dittrich, L., Beranek, V., Kotek, M., Schwarz, J., Vodicka, P., Milcova, A., Rossnerova, A.,
731 Ambroz, A., and Topinka, J.: Polycyclic aromatic hydrocarbons (PAH) and their genotoxicity in exhaust emissions from a
732 diesel engine during extended low-load operation on diesel and biodiesel fuels, *Atmos. Environ.*, 109, 9-18,
733 <https://doi.org/10.1016/j.atmosenv.2015.02.077>, 2015.

734 Wang, T., Quiros, D. C., Thiruvengadam, A., Pradhan, S., Hu, S., Huai, T., Lee, E. S., and Zhu, Y.: Total Particle Number
735 Emissions from Modern Diesel, Natural Gas, and Hybrid Heavy-Duty Vehicles During On-Road Operation, *Environ. Sci.*
736 *Technol.*, 51, 6990-6998, <https://doi.org/10.1021/acs.est.6b06464>, 2017.

737 Watne, A. K., Psichoudaki, M., Ljungstrom, E., Le Breton, M., Hallquist, M., Jerksjö, M., Fallgren, H., Jutterstrom, S., and
738 Hallquist, A. M.: Fresh and Oxidized Emissions from In-Use Transit Buses Running on Diesel, Biodiesel, and CNG, *Environ.*
739 *Sci. Technol.*, 52, 7720-7728, <https://doi.org/10.1021/acs.est.8b01394>, 2018.

740 Williams, M., and Minjares, R.: A technical summary of Euro 6/VI vehicle emission standards, International Council for Clean
741 Transportation (ICCT), Washington, DC, accessed July, 10, 2017, 2016.

742 Zavala, M., Molina, L. T., Yacovitch, T. I., Fortner, E. C., Roscioli, J. R., Floerchinger, C., Herndon, S. C., Kolb, C. E.,
743 Knighton, W. B., Paramo, V. H., Zirath, S., Mejia, J. A., and Jazcilevich, A.: Emission factors of black carbon and co-pollutants
744 from diesel vehicles in Mexico City, *Atmos. Chem. Phys.*, 17, 15293-15305, <https://doi.org/10.5194/acp-17-15293-2017>,
745 2017.

746 Zhang, S. J., Wu, Y., Liu, H., Huang, R. K., Yang, L. H. Z., Li, Z. H., Fu, L. X., and Hao, J. M.: Real-world fuel consumption
 747 and CO₂ emissions of urban public buses in Beijing, *Appl. Energ.*, 113, 1645-1655,
 748 <https://doi.org/10.1016/j.apenergy.2013.09.017>, 2014.

749 Zheng, Z., Johnson, K. C., Liu, Z., Durbin, T. D., Hu, S., Huai, T., Kittelson, D. B., and Jung, H. S.: Investigation of solid
 750 particle number measurement: Existence and nature of sub-23 nm particles under PMP methodology, *J. Aerosol Sci.*, 42, 883-
 751 897, <https://doi.org/10.1016/j.jaerosci.2011.08.003>, 2011.

752 Zheng, Z., Durbin, T. D., Xue, J., Johnson, K. C., Li, Y., Hu, S., Huai, T., Ayala, A., Kittelson, D. B., and Jung, H. S.:
 753 Comparison of particle mass and solid particle number (SPN) emissions from a heavy-duty diesel vehicle under on-road driving
 754 conditions and a standard testing cycle, *Environ. Sci. Technol.*, 48, 1779-1786, <https://doi.org/10.1021/es403578b>, 2014.

755 Zheng, Z. Q., Durbin, T. D., Karavalakis, G., Johnson, K. C., Chaudhary, A., Cocker, D. R., Herner, J. D., Robertson, W. H.,
 756 Huai, T., Ayala, A., Kittelson, D. B., and Jung, H. S.: Nature of Sub-23-nm Particles Downstream of the European Particle
 757 Measurement Programme (PMP)-Compliant System: A Real-Time Data Perspective, *Aerosol Sci. Tech.*, 46, 886-896,
 758 <https://doi.org/10.1080/02786826.2012.679167>, 2012.

759 Zhu, Y. F., Hinds, W. C., Kim, S., Shen, S., and Sioutas, C.: Study of ultrafine particles near a major highway with heavy-duty
 760 diesel traffic, *Atmos. Environ.*, 36, 4323-4335, [https://doi.org/10.1016/S1352-2310\(02\)00354-0](https://doi.org/10.1016/S1352-2310(02)00354-0), 2002.

761 **Table 1.** Comparison of the average emission data^a for PM and PN from the present study with literature data.

PM/PN						
Vehicle type	Speed km h ⁻¹	Dp range nm	Method	Instrument	EF _{PM} mg (kg fuel) ⁻¹	EF _{PN} # (kg fuel) ⁻¹ 10 ¹⁴
Euro III HDT in this study	26±6 ^b	5.6-560	roadside	EEPS	684±365	20.3±11.7
Euro III bus	acceleration	5.6-560	roadside	EEPS	6.7-2074	0.11-45
(Hallquist et al., 2013)	constant speed	5.6-560	roadside	EEPS	151-273	0.12-4.2
Euro III bus with DPF	acceleration	5.6-560	roadside	EEPS	62-2465	1.9-23
(Hallquist et al., 2013)	constant speed	5.6-560	roadside	EEPS	41-142	1.1-9.7
Euro III bus	≤25	PM ₁	plume chasing	ELPI ^c	1240±220 ^b	20.6±3.2 ^b
(Pirjola et al., 2016)	(bus depot)	D _p ≥2.5		CPC		
	≤45	PM ₁	plume chasing	ELPI ^c	500	17.7
	(bus line)	D _p ≥2.5		CPC		
Euro III bus with DPF+SCR	acceleration	5.6-560	roadside	EEPS	8.9±0.2	0.12±0.12
(Watne et al., 2018)						
Euro III bus with DPF+SCR	stop and go	5.6-560	roadside	EEPS	30±26 ^b	14.0±3.0 ^b
(Liu et al., 2019)	(bus stop)					
Euro III diesel bus and truck	driving cycle	35-1000	plume chasing & roadside	SP-AMS ^f	4300	-
(Zavala et al., 2017)						
Euro IV HDT in this study	23±8 ^b	5.6-560	roadside	EEPS	172±68	8.7±3.0
Euro IV bus with EGR	acceleration	5.6-560	roadside	EEPS	562-3089	13-44
(Hallquist et al., 2013)	constant speed	5.6-560	roadside	EEPS	91-489	5.8-47
Euro IV bus with EGR+DPF	acceleration	5.6-560	roadside	EEPS	177-650	5.1-13
(Hallquist et al., 2013)	constant speed	5.6-560	roadside	EEPS	58-61	2.6-3.1
Euro IV bus with EGR+DPF	≤25	PM ₁	plume chasing	ELPI ^c	1190±520 ^b	8.9±1.6 ^b
(Pirjola et al., 2016)	(bus depot)	D _p ≥2.5		CPC		
Euro IV bus with SCR	acceleration	5.6-560	roadside	EEPS	145-560	3-13
(Watne et al., 2018)						
Euro IV diesel bus and truck	driving cycle	35-1000	plume chasing and roadside	SP-AMS ^f	1800	-
(Zavala et al., 2017)						
Euro V HDT in this study	27±7 ^b	5.6-560	roadside	EEPS	146±49	9.7±2.7
Euro V bus+SCR	acceleration	5.6-560	roadside	EEPS	125-766	4.4-92
(Hallquist et al., 2013)	constant speed	5.6-560	roadside	EEPS	41-509	2.7-33
Euro V bus	acceleration	5.6-560	roadside	EEPS	145±70	3.0±1.7
(Watne et al., 2018)						
Euro V HDV with SCR	average at 45	PM/ 5.6-560	PEMS	MSS ^e	1840 ^d	0.09 ^d
(Rymaniak et al., 2017)				EEPS		
Euro V bus with SCR	stop and go	5.6-560	roadside	EEPS	180±15 ^b	6.5±2.9 ^b
(Liu et al., 2019)	(bus stop)					
Euro V diesel bus and truck	driving cycle	35-1000	plume chasing and roadside	SP-AMS ^f	720	-
(Zavala et al., 2017)						
EEV HDT in this study	25±8 ^b	5.6-560	roadside	EEPS	78±35	16.5±23.6

EEV bus with EGR +DPF (Pirjola et al., 2016)	≤25 (bus depot)	PM ₁ / D _p ≥2.5	plume chasing	ELPI ^c CPC	400±280 ^b	2.1±0.1 ^b
EEV bus with SCR (Pirjola et al., 2016)	≤25 (bus depot)	PM ₁ / D _p ≥2.5	plume chasing	ELPI ^c CPC	280±170 ^b	7.0±3.8 ^b
EEV with DOC+DPF+SCR (Rymaniak et al., 2017)	average at 45	PM/ 5.6-560	PEMS	MSS ^e EEPS	236 ^d	0.02 ^d
EEV bus (Jarvinen et al., 2019)	stop and go	PM ₁ / D _p ≥3	plume chasing	ELPI ^c CPC	200	8.6
Euro VI HDT in this study	29±8 ^b	5.6-560	roadside	EEPS	5±2	8.5±4.6
Euro VI bus (Jarvinen et al., 2019)	stop and go	PM ₁ / D _p ≥3	plume chasing	ELPI ^c CPC	70	5
Euro VI HDGV (Moody and Tate, 2017)	13-86	-	PEMS	-	28-33 ^d	-
Euro VI HDT (Grigoratos et al., 2019)	65-74	-	PEMS	-	-	0.002-0.01 ^d
<u>HDT without available Euro type information</u>	<u>27±7^b</u>	<u>5.6-560</u>	<u>roadside</u>	<u>EEPS</u>	<u>47±23</u>	<u>7.5±7.3</u>
<u>Total Swedish HDT</u>	<u>28±7^b</u>	<u>5.6-560</u>	<u>roadside</u>	<u>EEPS</u>	<u>96±36</u>	<u>9.6±2.7</u>
<u>Total non-Swedish HDT</u>	<u>26±8^b</u>	<u>5.6-560</u>	<u>roadside</u>	<u>EEPS</u>	<u>117±42</u>	<u>11.1±4.2</u>
<u>Non-European HDV with different ATS</u>						
HDV with DPF (Wang et al., 2017; Quiros et al., 2016)	13-80	PM D _p ≥5	PEMS	gravimetric CPC	12-41 ^d	0.006-13.2
Heavy-duty HDV with DPF+SCR (Thiruvengadam et al., 2015)	driving cycle	PM	chassis dynamometer	gravimetric	6-29 ^d	-
HDV with DPF+SCR (Jiang et al., 2018)	driving cycle	PM _{2.5}	chassis dynamometer	gravimetric	3-97 ^d	-
HDT (model year 2004- 2006) (Preble et al., 2015)	accelerating or cruise at 48	D _p ≥2.5	roadside	CPC	-	47.2±9.7
HDT with SCR+DPF (model year 2010- 2013) (Preble et al., 2015)		D _p ≥2.5	roadside	CPC	-	15.9±11.5
HDV (mean model year 2005) (Bishop et al., 2015)	15.7-16.8	PM _{1,2}	OHMS ^g	digital mass monitor	650	-
HDV (mean model year 2009) (Bishop et al., 2015)	7.7-9.3	PM _{1,2}	OHMS ^g	digital mass monitor	31	-
HDV without after-treatment (Quiros et al., 2018)	driving cycle	PM _{2.5}	chassis dynamometer	gravimetric	1980 ^d	-
HDV+DPF (Quiros et al., 2018)	driving cycle	PM _{2.5}	chassis dynamometer	gravimetric	6-9 ^d	-
<u>HDT without available Euro type information</u>	<u>27±7^b</u>	<u>5.6-560</u>	<u>roadside</u>	<u>EEPS</u>	<u>47±23</u>	<u>7.5±7.3</u>
<u>Total Swedish HDT</u>	<u>28±7^b</u>	<u>5.6-560</u>	<u>roadside</u>	<u>EEPS</u>	<u>96±36</u>	<u>9.6±2.7</u>
<u>Total non-Swedish HDT</u>	<u>26±8^b</u>	<u>5.6-560</u>	<u>roadside</u>	<u>EEPS</u>	<u>117±42</u>	<u>11.1±4.2</u>

762 ^a Given errors are at 95% CI.
763 ^b Standard deviation.
764 ^c ELPI, Electrical Low-Pressure Impactor.
765 ^d Average fuel consumption of 0.26 L km⁻¹ for HDV during long haul and regional delivery tests (Rexeis et al., 2018), the
766 density of 0.815 kg dm⁻³ (Swedish Environmental Protection Agency, 2013) of diesel particles were assumed for unit
767 conversion.
768 ^e MSS, Micro Soot Sensor.
769 ^f SP-AMS, Soot Particle Aerosol Mass Spectrometer.
770 ^g OHMS, On-Road Heavy-Duty Vehicle Emissions Monitoring System.

Vehicle type	Speed km h ⁻¹	Method	EF _{NO_x} ^b g (kg fuel) ⁻¹	EF _{NO₂} / EF _{NO_x} ^b mass ratio %	EF _{CO} ^c g (kg fuel) ⁻¹	EF _{HC} ^c g (kg fuel) ⁻¹
Euro III HDT in this study	26±6 ^d	roadside	43.3±31.5	7.5±4.1	36.0±13.2	0.8±1.3
Euro III bus (Hallquist et al., 2013)	acceleration	roadside	16.1±9.7	-	16.1±16.1	<13
Euro III bus (Pirjola et al., 2016)	≤25 (bus depot)	plume chasing	12.7±1.8 ^d	-	-	-
	≤45 (bus line)	plume chasing	20.5	-	-	-
Euro III bus with DPF+SCR (Watne et al., 2018)	acceleration	roadside	-	-	13±10	0.02
Euro III HDV (Lau et al., 2015)	64 ± 13 ^d	plume chasing	-	24±4	-	-
Euro III &IV HDV (Kousoulidou et al., 2008)	-	model	-	14	-	-
Euro III HGV (Carslaw et al., 2011)	Average at 31	remote sensing	16.2±1.0 ^f	-	-	-
Euro III HGV (Carslaw and Rhys-Tyler, 2013)	28-60	remote sensing	-	24.1±4.7	-	-
<u>Euro III HGV (Carslaw and Rhys-Tyler, 2013)</u>	<u>28-60</u>	<u>remote sensing</u>	<u>-</u>	<u>24.1±4.7</u>	<u>-</u>	<u>-</u>
Euro IV HDT in this study	23±8 ^d	roadside	19.8±10.1	2.7±2.9	22.1±10.3	0.7±1.1
Euro IV bus (Hallquist et al., 2013)	acceleration	roadside	12.9±6.5	-	16.1±16.1	<13
Euro IV bus with EGR+DPF (Pirjola et al., 2016)	≤25 (bus depot)	plume chasing	23.4±6.1 ^d	-	-	-
Euro IV bus with SCR (Watne et al., 2018)	roadside	acceleration	-	-	220-230	0.3-0.6
Euro IV HDV (Lau et al., 2015)	64 ± 13 ^d	plume chasing	-	28±5	-	-
Euro IV HGV (Carslaw et al., 2011)	average at 31	remote sensing	10.3±1.4 ^f	-	-	-
Euro IV HGV (Carslaw and Rhys-Tyler, 2013)	28-60	remote sensing	-	3.1±0.7	-	-
<u>Euro IV HGV (Carslaw and Rhys-Tyler, 2013)</u>	<u>28-60</u>	<u>remote sensing</u>	<u>-</u>	<u>3.1±0.7</u>	<u>-</u>	<u>-</u>
Euro V HDT in this study	27±7 ^d	roadside	22.2±3.8	6.0±2.8	22.8±5.1	0.9±0.4
Euro V bus (Hallquist et al., 2013)	acceleration	roadside	35.5±9.7	-	9.7±3.2	<13
Euro V bus with SCR (Liu et al., 2019)	stop and go (bus stop)	roadside	9.8±3.5 ^d	3.7±1.5 ^d	28 ^e	2.2 ^e
Euro V HDV (Lau et al., 2015)	64 ± 13 ^d	plume chasing	-	40±14	-	-
Euro V HDV (Kousoulidou et al., 2008)	-	model	-	18	-	-

Euro V HGV (Carslaw et al., 2011)	average at 31	remote sensing	13.3±5.8 ^f	-	-	-
Euro V HGV (Carslaw and Rhys-Tyler, 2013)	28-60	remote sensing	-	3.7±0.7	-	-
<u>Euro V HGV (Carslaw and Rhys-Tyler, 2013)</u>	<u>28-60</u>	<u>remote sensing</u>	<u>-</u>	<u>3.7±0.7</u>	<u>-</u>	<u>-</u>
EEV HDT in this study	25±8 ^d	roadside	13.6±6.7	6.3±3.7	18.0±10.1	0.2±0.4
EEV bus with EGR +DPF (Pirjola et al., 2016)	≤25 (bus depot)	plume chasing	32.9±7.6 ^d	-	-	-
EEV bus with SCR (Pirjola et al., 2016)	≤25 (bus depot)	plume chasing	39.8±4.2 ^d	-	-	-
Euro VI HDT in this study	29±8 ^d	roadside	3.1±1.0	22.5±4.2	15.5±2.2	1.0±0.5
Euro VI HDT (Grigoratos et al., 2019)	65-74	PEMS	0.3-31.3	-	2.8-22.3	0.3-3.1
Euro VI HDV (Kousoulidou et al., 2008)	-	model	-	35	-	-
Euro VI HDV (Moody and Tate, 2017)	driving cycle	PEMS	2.2 ^f	-	-	-
<u>HDT without available Euro type information</u>	<u>27±7^d</u>	<u>roadside</u>	<u>7.8±4.5</u>	<u>13.9±6.3</u>	<u>20.7±5.6</u>	<u>0.8±0.6</u>
<u>Total Swedish HDT</u>	<u>28±7^d</u>	<u>roadside</u>	<u>10.7±1.8</u>	<u>15.9±2.5</u>	<u>18.6±1.9</u>	<u>0.9±0.3</u>
<u>Total non-Swedish HDT</u>	<u>26±8^d</u>	<u>roadside</u>	<u>13.0±2.5</u>	<u>12.7±3.0</u>	<u>19.1±3.0</u>	<u>0.9±0.6</u>

Non-European HDV with different ATS

Heavy-duty HDV with DPF+SCR (Thiruvengadam et al., 2015)	driving cycle	chassis dynamometer	3.8-27.8 ^f	-	0.1-13.4 ^f	<0.64 ^f
HDV with DPF+SCR (Jiang et al., 2018)	driving cycle	chassis dynamometer	0.2-66.4 ^f	-	0.006- 14.9 ^f	<1.3 ^f
HDV with DOC+DPF+SCR (Quiros et al., 2016)	12.7-85.6	mobile laboratory	1.7-11.8 ^f	-	0.9-2.8 ^f	0.1-0.4 ^f
HDV (May et al., 2014)	driving cycle	chassis dynamometer	30-43	-	-	-
HDV with SCR (May et al., 2014)	driving cycle	chassis dynamometer	11	-	-	-
HDV fleet average (Haugen et al., 2018)	22.5±0.9	remote sensing	12.4±0.6	8.9	5.9±0.9	2.2±0.4
HDT (model year 2004- 2006) (Preble et al., 2015)	accelerating or cruise at 48	roadside	16.5±1.7	3.4±1.8	-	-
HDT with SCR+DPF (model year 2010- 2013) (Preble et al., 2015)	48	roadside	5.1±1.2	22.1±8.4	-	-
HDT (model year 2001) (Burgard et al., 2006)	5-25	roadside	-	9.1±0.5	26.0±2.1	1.8±0.6
HDT (model year 2000) (Burgard et al., 2006)	20-40	roadside	-	6.1±0.1	37.9±1.6	3.3±0.4

Fleet average in 2006 (Bishop and Stedman, 2008)	28-36	roadside	2-5	-	17-24	1.9-2.3
HDT fleet average (Dallmann et al., 2012)	65	roadside	28±1.5	7.0	8.0±1.2	-
HDT (mean model year 2004) (Bishop et al., 2013)	22.2±0.4	remote sensing	20.6±0.6 ^d	9.7	8.2±0.6 ^d	3.7±0.1 ^d
HDT (mean model year 2009) (Bishop et al., 2013)	7.8±0.1	remote sensing	19.9±0.3 ^d	9.0	7.3±0.5 ^d	0.6±0.6 ^d
HDT without available Euro type information	27±7^d	roadside	7.8±4.5	13.9±6.3	20.7±5.6	0.8±0.6
Total Swedish HDT	28±7^d	roadside	10.7±1.8	15.9±2.5	18.6±1.9	0.9±0.3
Total non-Swedish HDT	26±8^d	roadside	13.0±2.5	12.7±3.0	19.1±3.0	0.9±0.6

^a Given errors are at 95% CI.

^b In NO₂ equivalents.

^c RSD data. For the RSD data sets of multiple individuals, negative values were replaced by zero when calculating the averages.

^d Standard deviation.

^e Median.

^f Average fuel consumption of 0.26 L km⁻¹ for HDV during long haul and regional delivery tests (Rexeis et al., 2018), the density of 0.815 kg dm⁻³ (Swedish Environmental Protection Agency, 2013) of diesel particles were assumed.

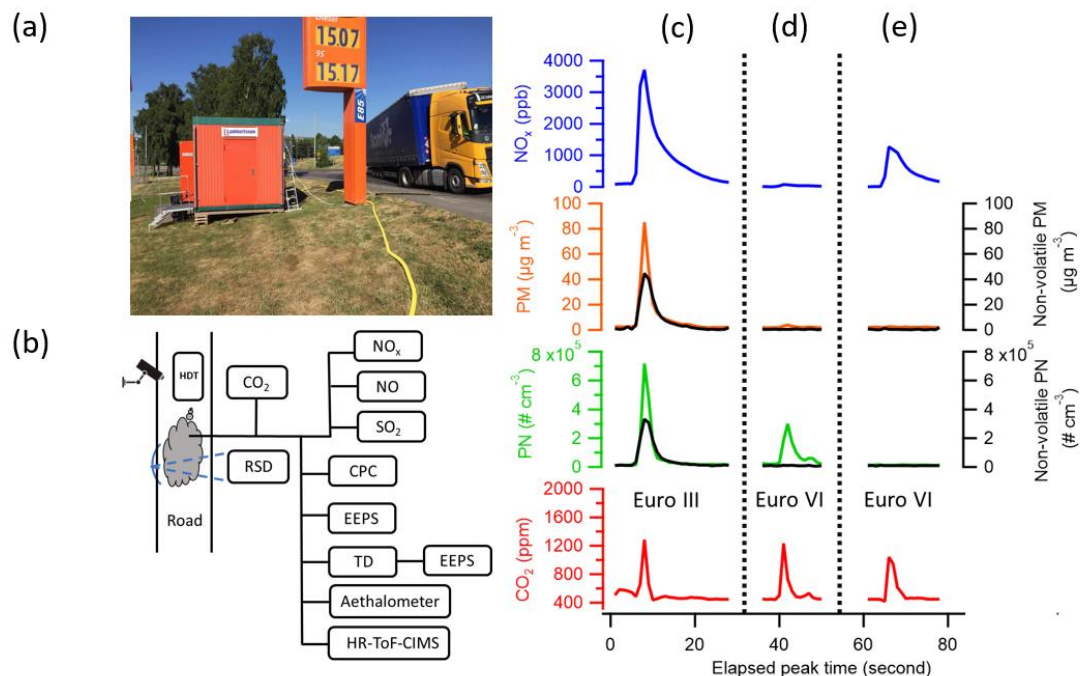


Figure 1. (a) Sampling site at the roadside in Gothenburg, Sweden, (b) schematic of the experimental set-up. HDT (Heavy-duty truck), RSD (Remote Sensing Device), CPC (Condensation Particle Counter), EEPS (Engine Exhaust Particle Sizer Spectrometer), TD (Thermodenuder) and HR-ToF-CIMS* (High-Resolution Time-of-Flight Chemical Ionization Mass Spectrometer) and examples of signals from three passing HDTs. Concentrations of CO₂, PN, non-volatile PN (black line), PM, non-volatile PM (black line), and NO_x from (c) a typical Euro III HDT and (d) a typical Euro VI HDT and (e) a Euro VI HDT with low PN emission. *The data from the HR-ToF-CIMS will be presented elsewhere.

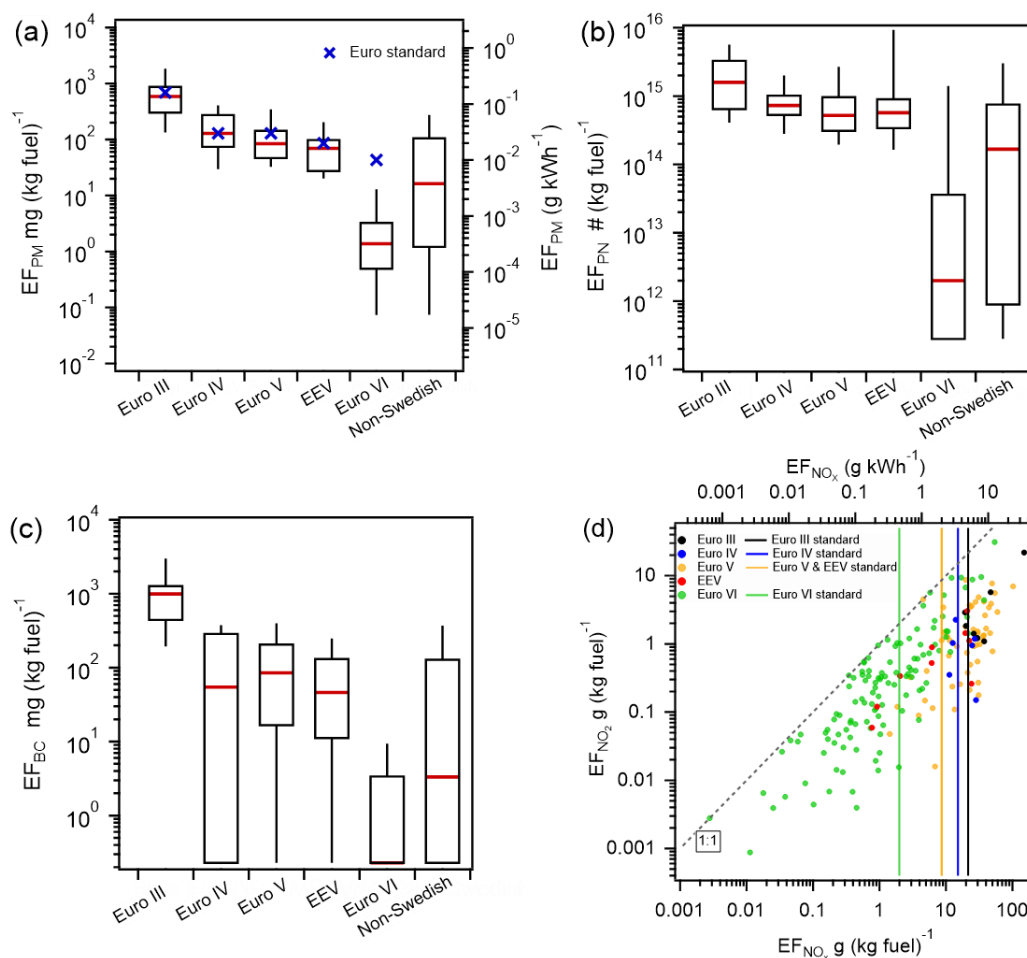


Figure 2. (a) EF_{PM} , (b) EF_{PN} , (c) EF_{BC} , (d) EF_{NO_2} and EF_{NO_x} for Euro III to Euro VI and non-Swedish HDTs. Non-detectable pollutant emission signals for captured plumes have been replaced by EF_{min} . For box-and-whisker plots, the top and the bottom line of the box are 75th and 25th percentiles of the data, the red line inside the box is the median, and the top and bottom whiskers are 90th and 10th percentiles. EF_{NO_x} in (d) are in NO_2 equivalents. HDTs with either EF_{NO_2} or EF_{NO_x} lower than the detection limits of the instruments were removed in (d) for illustration purposes. Note that the comparison with the emission standard is only indicative as they are based on test cycle performance.

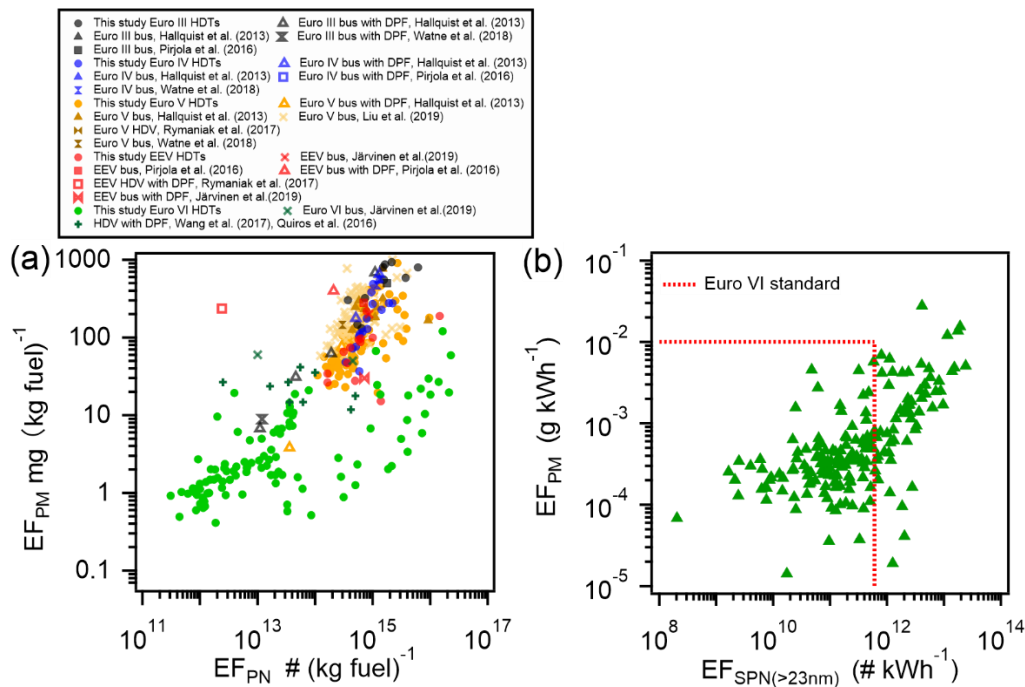


Figure 3. (a) EF_{PM} and EF_{PN} of individual HDTs in this study and previous studies and (b) the relationship between EF_{PM} and EF_{SPN} of Euro VI HDTs. Red dashed lines represent Euro emission standards (horizontal: PM emission standard; vertical: SPN emission standard). HDTs with either EF_{PM} or EF_{PN} lower than the detection limits of the instruments were removed in (a) for illustration purposes. Note that the comparison with the emission standard is only indicative as they are based on test cycle performance.

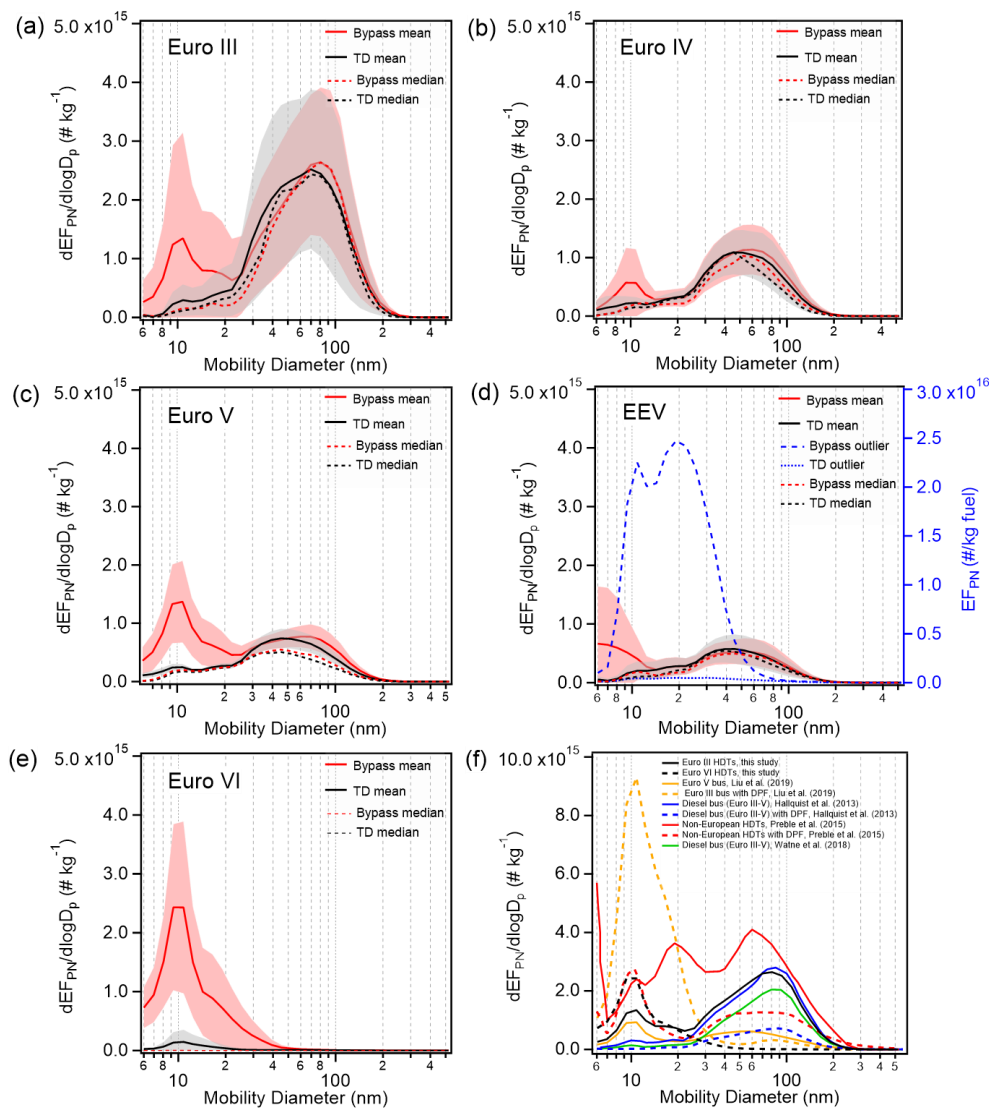


Figure 4. (a-e) Mean and median size-resolved EF_{PN} and $EF_{non-volatile\ PN}$ of different Euro class HDTs and (f) comparisons of mean size-resolved EF_{PN} of HDVs in this study and previous studies. Shaded regions in (a-e) represent the statistical 95% confidence interval. One HDT with extremely different EF in (d) was excluded and shown in blue.

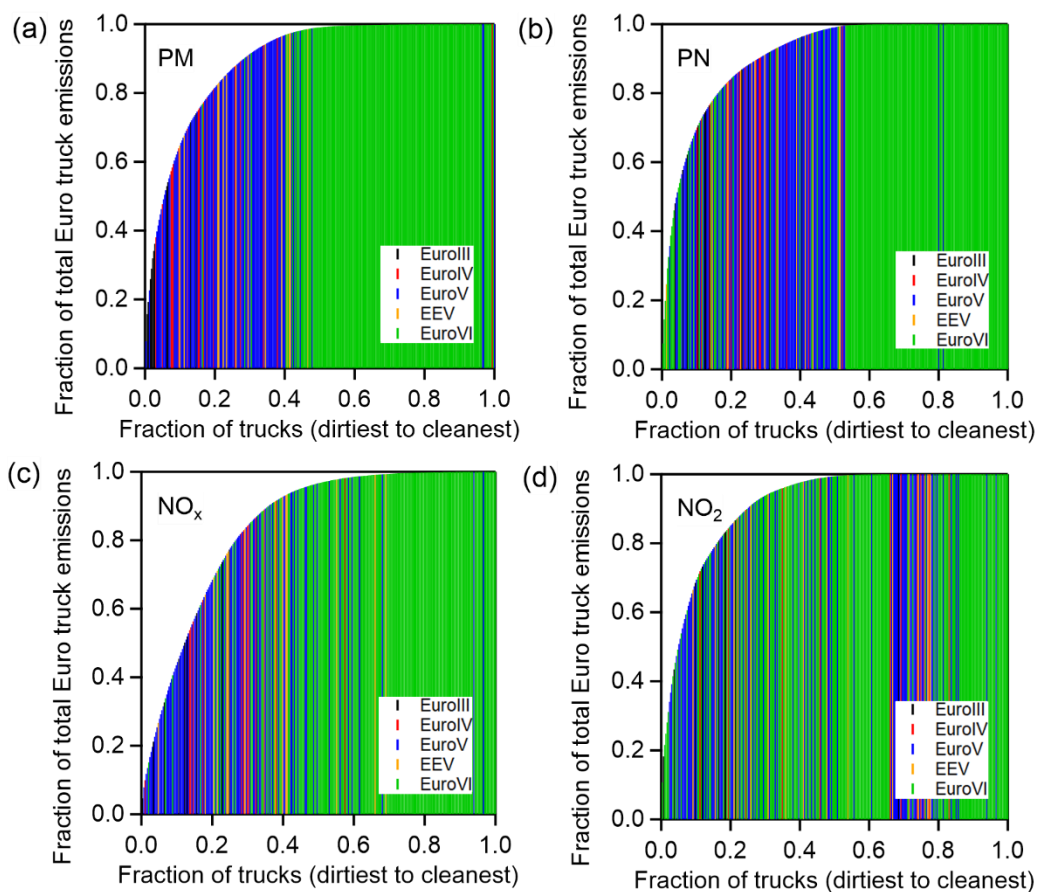


Figure 5. Cumulative emission factor distribution for (a) PM, (b) PN, (c) NO_x, and (d) NO₂ measured in HDT exhaust plumes with HDTs ranked from the highest to lowest in terms of emission factors.

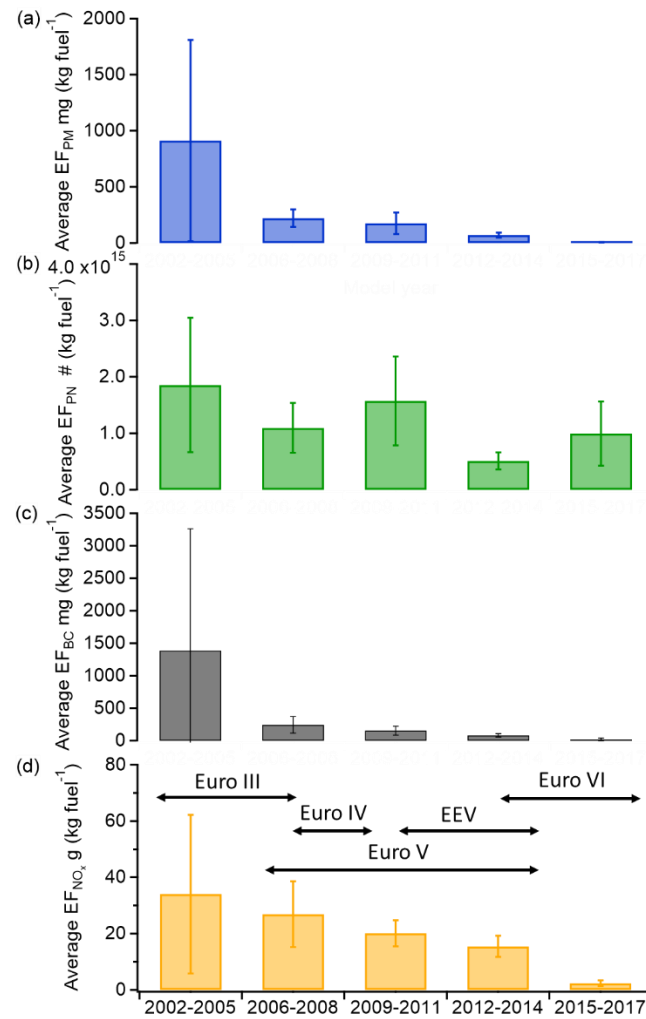


Figure 6. Changes of average EFs of (a) PM, (b) PN, (c) BC and (d) NO_x with respect to the registration year of HDTs. Error bars represent the statistical 95% confidence interval. Black arrows mark the years that the particular type of HDT examined in this study was first registered.

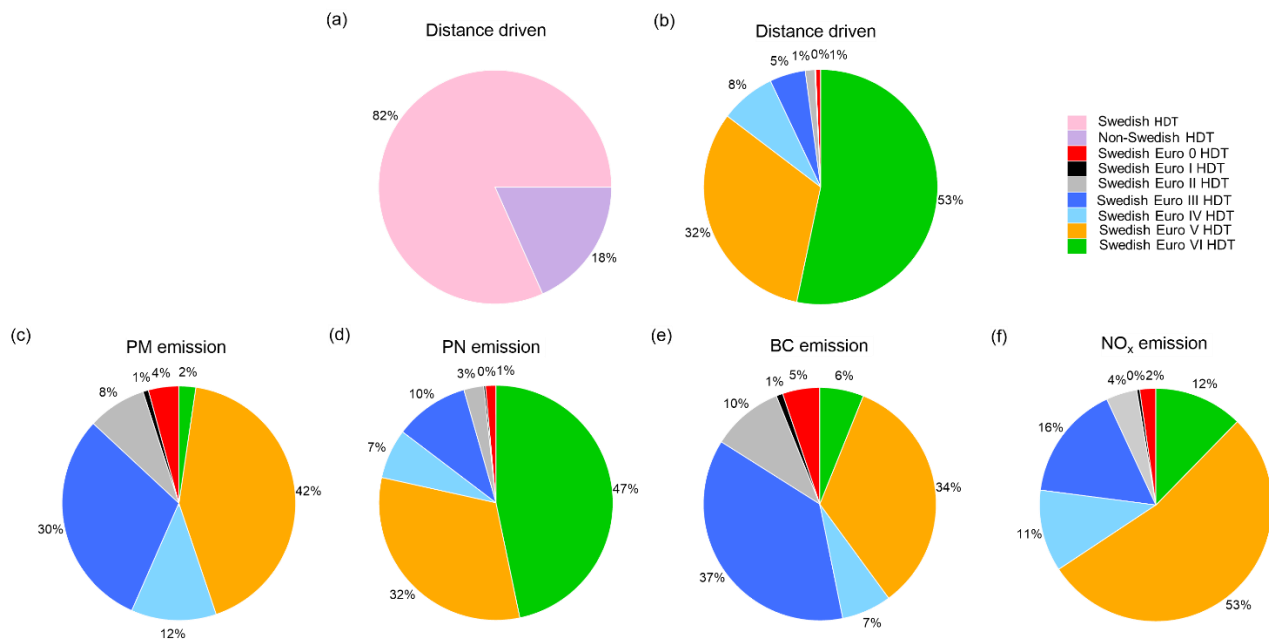


Figure 7. Relative contributions of kilometers driven by (a) Swedish and Non-Swedish HDTs and (b) Swedish Euro 0, Euro I, Euro II, Euro III, Euro IV, Euro V and Euro VI HDTs on Swedish roads during 2018. Approximation of contributions of pollutants emitted from Swedish HDTs in each Euro class to the total (c) PM, (d) PN, (e) BC and (f) NO_x emissions.